

# Pointer States via Engineered Dissipation

Kaveh Khodjasteh,<sup>1</sup> Viatcheslav V. Dobrovitski,<sup>2</sup> and Lorenza Viola<sup>1</sup>

<sup>1</sup>*Department of Physics and Astronomy, Dartmouth College, Hanover, NH 03755, USA*

<sup>2</sup>*Ames Laboratory, Iowa State University, Ames, IA 50011, USA*

(Dated: November 26, 2024)

Pointer states are long-lasting high-fidelity states in open quantum systems. We show how any pure state in a non-Markovian open quantum system can be made to behave as a pointer state by suitably engineering the coupling to the environment via open-loop periodic control. Engineered pointer states are constructed as *approximate fixed points* of the controlled open-system dynamics, in such a way that they are *guaranteed* to survive over a long time with a fidelity determined by the relative precision with which the dynamics is engineered. We provide quantitative minimum-fidelity bounds by identifying symmetry and ergodicity conditions that the decoherence-inducing perturbation must obey in the presence of control, and develop explicit pulse sequences for engineering any desired set of orthogonal states as pointer states. These general control protocols are validated through exact numerical simulations as well as semi-classical approximations in realistic single- and two- qubit dissipative systems. We also examine the role of control imperfections, and show that while pointer-state engineering protocols are highly robust in the presence of systematic pulse errors, the latter can also lead to unintended pointer-state generation in dynamical decoupling implementations, explaining the initial-state selectivity observed in recent experiments.

PACS numbers: 03.67.Pp, 03.65.Yz, 07.05.Dz

## I. INTRODUCTION

Understanding how and to what extent robust classical properties can dynamically emerge in open quantum systems as a result of the unavoidable interaction with the surrounding environment has long been identified as a problem of central significance to quantum physics and quantum engineering. The concept of *pointer states* (PSs) has been introduced by Zurek [1] to capture the fact that not all initial pure states of an open quantum system may be equally fragile with respect to the interaction with the environment: PSs are distinguished by their ability to persist with high fidelity over time scales of practical interest, and are thus natural candidates to describe “preferred” states in which open quantum systems are found in reality. As a result, PSs play a fundamental role in investigations of the quantum-to-classical transition and quantum measurement models [2], as well as of general aspects of “most classical” minimum-uncertainty states in quantum-dynamical systems [3–6]. In the context of quantum information processing, a set of mutually orthogonal PSs (a *pointer basis*) provides the simplest example of an “information-preserving structure” (IPS) [7]: since arbitrary convex mixtures of PSs are preserved, a pointer basis naturally realizes a robust *classical memory*. As a result, PSs are also practically attractive in view of their potential for long-lasting storage capabilities.

From a physical standpoint, the robustness of PSs can be traced back to the fact that they become “least entangled” with the environment in the course of the dynamics [1]. Mathematically (in a sense that will be made more precise later), this is only possible if the open-system Hamiltonian exhibits a sufficient degree of *symmetry*, which effectively allows PSs to be eigenstates (fixed points [7]) in the resulting system-plus-bath di-

lation. This has two implications: On the one hand, for a *generic* open quantum system, such a symmetry is *not* typical and at best approximate, thus PSs need not exist – with all the initial preparations of the system being rapidly degraded over comparable time scales. On the other hand, even in situations where a robust set of states would be naturally “ein-selected” over time, the latter would be inflexibly determined by the Hamiltonian under consideration – with the resulting PSs not necessarily coinciding with states of interest, and with no control over their actual fidelity and lifetime. By reversing this logic, we may then ask whether by suitably “engineering dissipation”, that is, by resorting to external manipulation and perfection of the symmetry in the controlled open-system Hamiltonian, it is possible to make *any target set of initial pure states into artificial PSs*, so that the desired initial preparations can be robustly stored over time and their features retrieved on demand. This is the question that will be addressed and constructively answered in this paper – a task to which we refer to as “pointer state engineering”.

Our strategy relies on open-loop (feedback-free) quantum control methods, close in spirit to dynamical decoupling (DD) approaches to decoherence suppression [8–16] and robust quantum computation [17–20]. The idea is to start from the “bare” open-system Hamiltonian that describes the interaction between the system and its environment, and to incorporate this Hamiltonian along into a pre-designated control recipe that acts directly *only* on the system, either in the form of sufficiently fast sequences of control pulses or continuous time-dependent modulation. Since in practice only limited knowledge of the bath degrees of freedom may be available, an important requirement in DD constructions is that they be robust against variations in the bath op-

erators, and determined only by algebraic properties of the underlying open-system Hamiltonian. While a variety of different protocols exist (and are being successfully tested in the laboratory [21, 22]), their common aim is the synthesis, perfection, and upkeep of an effective Hamiltonian which is “dynamically symmetrized”, so that interactions with the environment are *removed*, up to a given order of accuracy, for the evolution of any state inside the entire system’s Hilbert space [9, 10] or within a (control-dependent) “dynamically generated” decoherence-free subspace or noiseless subsystem [23, 24]. Technically, this is achieved via a number of algebraic techniques for manipulating generic interaction Hamiltonians, along with analytic approaches for perturbatively (or numerically [25–27]) reducing the unwanted decoherence contributions and bounding the residual errors.

While many of the building blocks used in the design and analysis of DD protocols will also be employed for the task of engineering PSs, it is important to clarify how the two problems differ. In a typical DD setting, the goal is to synthesize, for a given system-bath Hamiltonian, a target unitary propagator (the identity evolution) on the system with a sufficiently high gate fidelity, so that, ideally, *arbitrary initial preparations* can be robustly preserved over a desired storage time (or stroboscopically in time if the DD cycle is repeated). As a consequence, in a good DD scheme the control performance should be as *unbiased* as possible with respect to different initializations, and DD protocols must be constructed without making reference to and/or taking advantage of possible knowledge of the system’s initial state. While the system-bath Hamiltonian is also given in the PS-engineering problem, the target set of initial preparations to be preserved is also specified as an additional input. Thus, knowledge of this target set should be explicitly incorporated into designing a good PS-protocol, so that the output fidelity is *optimized* for the desired PSs over the desired storage time. These differences result in important practical advantages: while DD methods discovered so far can in fact only guarantee a reduced fidelity *decay rate* over time, in PS-engineering we will be able to guarantee a high fidelity *value* over long time-spans. The end result is that the designated states can live much longer (in principle as long as desired) in a PS-engineering scheme rather than in general DD procedures intended for quantum memory.

A few remarks may be useful to further place our work in context. First, we note that, interestingly, high-order/uncanceled corrections to effective Hamiltonians in DD constructions may contain an additional degree of symmetry (with respect to the minimum needed to ensure the intended averaging of the system-bath interaction) and thus result in the generation of “accidental” PSs – and effective *decoherence freezing*, as predicted in [28, 29]. Remarkably, such accidental PSs have been observed in recent DD experiments [22, 30]. While the physical mechanism responsible for the observed initial-state-sensitivity is different than in a PS-engineering protocol (stemming, in the experiment, from systematic pulse er-

rors), we shall also address the emergence of such accidental PSs in DD sequences and show how they may be formally related within a unified control-theoretic framework. Second, we also iterate that DD has been invoked as a general strategy for generating IPSs in (non-Markovian) open quantum systems – decoherence-free subspaces and noiseless subsystem [23, 24], which can both be seen as multi-dimensional generalizations of PSs in an appropriate sense [7]. Again, a key difference is that such schemes are not tailored to preserve a target subspace or subsystem specified in advance. In this sense, our present analysis shares some motivation with (closed-loop) stabilization protocols for Markovian evolutions [31–33], restricted however to purely unitary control resources and to the (simplest) case of *discrete* sets of states (*classical* IPS) in the system Hilbert space. Lastly, we recall that the possibility of a prolonged high-fidelity regime – so-called *quantum fidelity freeze* – has been extensively analyzed in the context of Loschmidt echoes for closed quantum systems evolving under a *vanishing* time-averaged perturbation [34–36] and, in turn, shown to be intimately related to DD [37]. From this point of view, PS engineering may be interpreted as dynamically providing the requirements for a stronger freeze phenomenon to emerge, in generic open quantum systems, for the target set of initial preparations of interest.

The content of this paper is organized as follows. In Sec. II, we describe the general control setting, along with the algebraic conditions required for the effective controlled Hamiltonian to admit PSs. In Sec. III we characterize the effect that the unavoidable deviation of the actual effective Hamiltonian from the intended PS-supporting form implies on the quality of the engineered PSs. Our main result is a quantitative lower bound for the minimum fidelity which can be guaranteed for the PSs over a range of storage times in terms of both spectral/locality properties of the open-system Hamiltonian and details of the applied control scheme. Constructive protocols for engineering an arbitrary set of PSs are described in Sec. IV, whereas explicit illustrations in paradigmatic control scenarios are given in Sec. V based on both semiclassical analytical results and exact numerical simulations. In particular, single-qubit sequences are analyzed and contrasted to DD sequences resulting in accidental PSs, and sequences for engineering Bell states as PSs in two exchange-coupled qubits are presented, recovering and extending partial results in [38]. Sec. VI addresses the impact of limited control as resulting from imperfect initialization capabilities and/or imperfect control operations. We both characterize the degree of robustness of the PS-engineering sequences against systematic control errors, and, conversely, show how such control errors can result in accidental PSs in realistic DD sequences. Sec. VIII concludes with a summary of our main results, along with a discussion of their possible implications and further open problems.

## II. NOTATION AND PROBLEM SETUP

Throughout this work, we focus on a finite-dimensional open quantum system, that is, a distinguished subsystem  $S$  with associated  $D_S$ -dimensional Hilbert space  $\mathcal{H}_S$ , coupled to an environment (or bath)  $B$ , with associated  $D_B$ -dimensional Hilbert space  $\mathcal{H}_B$  [39]. We use  $|j\rangle$  to refer to system states and  $|b\rangle$  to refer to bath states, the overall composite Hilbert space being given by  $\mathcal{H}_S \otimes \mathcal{H}_B$ . For a product state  $|j\rangle \otimes |b\rangle$ , we refer to  $|j\rangle$  ( $|b\rangle$ ) as the system (bath) component, respectively. A factorizable density operator will have system and bath components in a similar way. Unless otherwise stated, we choose units in which  $\hbar = 1$ . We also tend to drop trivial tensor product signs, identity operators on  $S$  ( $I_S$ ) or  $B$  ( $I_B$ ), and ignore ordering of commuting operators as long as there is no ambiguity. Finally, we use the asymptotic notation with respect to operators in a lax manner. For example,  $A + O(\epsilon)$  might refer to an operator  $A$  plus corrections whose norm (such as the maximum singular value norm) is  $O(\epsilon)$ . In perturbation theory,  $O(x)$  will symbolically denote corrections that scale linearly with a quantity  $x$  which need not be dimensionless.

The joint evolution of the system and the environment is taken to be generated by a Hamiltonian of the form

$$H(t) = H_0 + H_{\text{ctrl}}(t).$$

Here,  $H_{\text{ctrl}}(t)$  is a controllable Hamiltonian that acts non-trivially only on  $\mathcal{H}_S$  and that shall be employed for generating unitary operations, whereas the free Hamiltonian  $H_0$  is specified in a frame where no explicit time-dependence is present and can be further expressed as

$$\begin{aligned} H_0 &= H_{SB} + I_S \otimes H_B \\ &\equiv H_S \otimes I_B + H'_{SB} + I_S \otimes H_B. \end{aligned} \quad (1)$$

That is,  $H_B$  denotes the internal evolution of the bath, and  $H_{SB}$  denotes the interaction Hamiltonian between  $S$  and  $B$ , including the internal evolution  $H_S$  of  $S$ . Formally, the latter can be isolated by demanding that  $H'_{SB}$  involves only traceless operators on  $B$ . In this way, the limit of a closed (unitarily evolving) quantum system is recovered for  $H'_{SB} = 0$  (thus  $H_{SB} \equiv H_S$ ). The limit where the bath is treated semi-classically corresponds instead to  $\mathcal{H}_B \simeq \mathbb{C}$  and the net effect of  $H_{SB}$  is a random modification of the system Hamiltonian, hence formally  $H_{SB}$  acts on  $\mathcal{H}_S$  only [40].

Our goal is to use open-loop control, specifically through the application of a pre-determined  $H_{\text{ctrl}}(t)$ , to enhance and maintain the fidelity of an arbitrary target set of orthogonal PSs. The strategy we follow is to modify the evolution of the composite system by subjecting it to *repeated identical control cycles*. Let the evolution propagator for each period (cycle) of the controlled evolution be denoted by  $U_c$ . Our fundamental assumption is that the cycle propagator  $U_c$ , no matter how implemented, remains the same for all cycles applied. Suppose that the

duration of each cycle is  $T_c$  and  $N$  repetitions are implemented, up to the total time  $T = NT_c$ , with  $N$  integer. Then the cycle propagator  $U_c$  defines an effective cycle Hamiltonian  $H_c$  on  $\mathcal{H}_S \otimes \mathcal{H}_B$  with the following structure:

$$\begin{aligned} U_c(T_c) &\equiv U_c = \exp[-iT_c H_c], \\ H_c &= H_{SB,c} + I_S \otimes H_{B,c}, \end{aligned} \quad (2)$$

where, in analogy with Eq. (1),  $H_{B,c}$  acts as an internal bath Hamiltonian and  $H_{SB,c}$  as a system-bath interaction, respectively. We emphasize that  $H_{SB,c}$  and  $H_{B,c}$  are *not*, in general, the same that appear in the bare interaction in Eq. (1). In fact,  $H_{SB,c}$  can be made much smaller than  $H_{SB}$  in DD, whereas pure-bath terms may be induced by the control even for a “non-dynamical” bath, for which the bare Hamiltonian  $H_B = 0$ . The periodicity of the evolution allows us to obtain a time-independent effective Hamiltonian  $H_c$ , since stroboscopically the evolution is given by

$$U_N(T) \equiv U_N = (U_c)^N = \exp[-iT H_c].$$

The key to achieve our control objective is to design  $H_{\text{ctrl}}(t)$  in such a way that  $H_{SB,c}$  takes a special form that we define next. The actual control schemes that result in this special form will be given in Sec. IV.

Let the orthonormal set of states  $\{|j\rangle\}_{j=0}^{p-1}$  ( $p \leq D_S$ ) denote our target PSs. The basic step is to ensure that  $H_{SB,c}$  is expressible in terms of a *dominant* operator  $H_{\text{dom}}$  and a *perturbation*  $\epsilon H_{\text{per}}$ , such that

$$\begin{aligned} H_{SB,c}(\epsilon) &= H_{\text{dom}} + \epsilon H_{\text{per}}, \\ H_{\text{dom}} &= \sum_{j=0}^{p-1} |j\rangle\langle j| \otimes B_j + H', \end{aligned} \quad (3)$$

where  $H'$  annihilates  $\text{Span}\{|j\rangle_{j=0}^{p-1}\}$  and  $B_j$  are distinct but otherwise arbitrary operators on  $B$ . This dependence of bath operators upon  $j$  is crucial to ensure that in the limit where  $\epsilon \rightarrow 0$ , each  $|j\rangle$  (but no coherent superposition) is *invariant* under evolution generated by  $H_c$ . Accordingly, we shall also refer to Eq. (3) as the “PS condition” henceforth. For nonvanishing  $\epsilon$ , the term  $\epsilon H_{\text{per}}$  is, in general, a system-bath Hermitian operator. Without loss of generality, we can shift any diagonal contribution of  $H_{\text{per}}$  in the PS basis into  $H_{\text{dom}}$ , so that [41]

$$\langle j|H_{\text{per}}|j\rangle = 0, \quad \forall j. \quad (4)$$

Note that if all but one PSs appear in the sum in Eq. (3), the remaining state will automatically become part of the sum also, implying the equivalence of  $p = D_S - 1$  and  $p = D_S$ . If  $p < D_S - 1$ , the system Hilbert space is decomposed into two orthogonal subspaces, one generated by the PS set  $\{|j\rangle\}_{j=0}^{p-1}$ , and the rest. Beyond Eq. (3) and requiring  $\epsilon$  to be sufficiently small, we need not specify the controlled effective Hamiltonian further.

Clearly, if the perturbation  $\epsilon H_{\text{per}}$  was zero, and the system was initialized in any of the PSs, each of these

states would be indefinitely preserved with maximal fidelity over time, just as the energy eigenstates in a closed-system setting. Realistically, however, even with sophisticated control schemes, the correction  $\epsilon H_{\text{per}}$  cannot in general be avoided. A good control scheme should ensure that the states  $\{|j\rangle\}_{j=0}^{p-1}$  are still singled out for their high-fidelity evolution, and can thus play the role of *engineered PSs*. Prior to providing explicit control schemes that synthesize effective Hamiltonians close to  $H_{\text{dom}}$ , we need to know how the corrections will affect the survival of the desired PSs in order to be able to maintain their performance. We thus proceed to analyze the extent to which the fate of the engineered PSs is modified in the presence of the inevitable correction terms.

### III. FIDELITY DYNAMICS OF ENGINEERED POINTER STATES

As a basic motivating example, consider a two-level system, in which  $H_{\text{dom}}$  is perturbed by a fixed intra-level coupling  $\epsilon H_{\text{per}}$ . If the energy levels are non-degenerate, the eigenstates of the *unperturbed* Hamiltonian  $H_{\text{dom}}$  can be seen as perturbations of the eigenstates of the *perturbed* Hamiltonian. Similar to the familiar Rabi problem, the discrepancy between the eigenstates is controlled by the *ratio* of the transition term to the energy gap and sets the amplitude of the oscillations that will ensue. For a degenerate system, the unperturbed eigenstates can end up being very far from the perturbed eigenstates and thus oscillate with a large amplitude [42, p. 194]. The eigenstates of the original unperturbed Hamiltonian  $H_{\text{dom}}$  thus play the role of PSs which retain their high fidelity (modulo some oscillation) under perturbation.

In an open-system setting, we shall use a similar idea with some modifications. The eigenstates of a perturbed system-bath Hamiltonian will still be close to the unperturbed eigenstates as long as there is no degeneracy, but the actual difference between the eigenstates is expanded over the composite Hilbert space which can sample over many basis states. The fidelity distance will thus need to reflect the larger size of the composite system-bath Hilbert space. This distance argument can be modified using an ergodic argument to yield a tighter fidelity bound for the pointer basis elements.

#### A. Semi-Classical Environment

Consider first a semi-classical setting in which, formally,  $H_{B,c} = 0$  and  $H_{SB,c}$  is a *system* operator. Let  $\{|j(\epsilon)\rangle\}_{k=0}^{D_S-1}$  denote the (perturbed) normalized eigenstates of  $H_{SB,c}(\epsilon) = H_{\text{dom}} + \epsilon H_{\text{per}}$ , with eigenvalues  $\omega_j(\epsilon)$ . Thus,  $\lim_{\epsilon \rightarrow 0} |j(\epsilon)\rangle = |j\rangle$  and  $\lim_{\epsilon \rightarrow 0} \omega_j(\epsilon) = \omega_j$ , where, without loss of generality, we may let  $\omega_0(0) \equiv 0$ .

Focus for simplicity on the preservation of a single PS, say  $|0\rangle$ . The system starts at  $\rho_S(0) = |0\rangle\langle 0|$  and after  $N$  cycles evolves to  $\rho_S(N) = U_c^N \rho_S(0) U_c^{-N}$ . A convenient

metric for quantifying the distance between  $\rho_S(0)$  and  $\rho_S(N)$  is the survival probability (or input-output fidelity [43]), given by

$$f_N \equiv \text{Tr}[\rho_S(0)\rho_S(N)] = \langle 0|\rho_S(N)|0\rangle,$$

which, since  $\rho_S(0)$  is pure, is simply related to the corresponding Uhlmann's fidelity  $f_N^U$  via  $f_N = (f_N^U)^2$ . The initial state  $|0\rangle$  will oscillate as a function of  $N$  with frequencies given by  $T_c \omega_j(\epsilon)$ . In the absence of degeneracy (for  $\omega_0$ ), the amplitude of oscillation is determined by the difference between  $|0\rangle$  and  $|0(\epsilon)\rangle$  and is thus controlled by  $\epsilon$  through the ratio of the perturbation to the dominant term. More precisely, upon expanding  $|0\rangle$  in the  $\{|k(\epsilon)\rangle\}$  basis and applying  $U_c^N$ , the fidelity loss reads as

$$1 - f_N = 1 - \left| \sum_j e^{-iNT_c \omega_j(\epsilon)} |\langle 0|j(\epsilon)\rangle|^2 \right|^2. \quad (5)$$

In the regime where  $\epsilon$  is sufficiently small, the required probability overlap (note that  $|\langle j|j(\epsilon)\rangle|^2$  is the so-called local density of states [37]) can be estimated using standard 1st order non-degenerate perturbation theory,

$$\begin{cases} |j(\epsilon)\rangle = Z_j^{1/2} \left( |j\rangle + \epsilon \sum_{n \neq j} |n\rangle \frac{\langle n|H_{\text{per}}|j\rangle}{\omega_j - \omega_n} \right), \\ Z_j \approx 1 - \epsilon^2 \sum_{n \neq j} \frac{|\langle n|H_{\text{per}}|j\rangle|^2}{(\omega_j - \omega_n)^2}, \end{cases}$$

yielding

$$|\langle 0|j(\epsilon)\rangle|^2 \approx \begin{cases} Z_j, & j = 0, \\ \epsilon^2 |\langle 0|H_{\text{per}}|j\rangle|^2 / \omega_j^2, & j \neq 0. \end{cases}$$

Upon substituting the above expression in Eq. (5) and retaining terms up to order  $O(\epsilon^2)$ , one finds

$$1 - f_N \approx \epsilon^2 \sum_{j \neq 0} 4 \sin^2[NT_c \omega_j/2] \frac{|\langle 0|H_{\text{per}}|j\rangle|^2}{\omega_j^2}.$$

Under the perturbative assumption that  $|\langle 0|H_{\text{per}}|j\rangle/\omega_j|$  is sufficiently small for all  $j \neq 0$ , this finally results in the desired (uniform) fidelity lower bound:

$$f_N \gtrsim 1 - 4\epsilon^2 D_S \max_{j \neq 0} \frac{|\langle 0|H_{\text{per}}|j\rangle|^2}{\omega_j^2}. \quad (6)$$

As noted, if a degeneracy exists in  $H_{\text{dom}}$ , the maximum fidelity loss cannot be bounded by a smooth function of  $\epsilon$ , since  $|0(\epsilon)\rangle$  and  $|0\rangle$  can be far apart *regardless* of  $\epsilon$  and at some point the initial state may oscillate too far and become completely lost.

In the absence of degeneracy, Eq. (6) points to an elementary yet remarkable feature: no matter how long the time passed since preparation, *the fidelity loss for an approximate eigenstate is small and bounded*. This is a crucial property of PSs and one that we will strive to reproduce in the general quantum case. As it turns out, the fidelity dynamics of an engineered PS in the presence of a quantum environment will closely follow the above

perturbative derivation. Furthermore, the semiclassical approximation may be of independent interest in realistic settings. For example, under appropriate physical and time-scale conditions, the contact hyperfine interaction of localized electronic spins with the surrounding nuclear-spin bath in semiconductors can be modeled in terms of a static but inhomogeneous magnetic field as long as ensemble measurements are considered [30, 44–48]. Our semiclassical analysis transcribes perfectly to this setting.

Let us focus, in particular, on a two-level system, and let  $\sigma_\alpha$ ,  $\alpha = x, y, z$ , denote the corresponding Pauli matrices. In the semiclassical limit, let

$$H_{SB} = \vec{\mathbf{b}} \cdot \vec{\sigma} \equiv b_x \sigma_x + b_y \sigma_y + b_z \sigma_z,$$

where  $\vec{\mathbf{b}} = (b_x, b_y, b_z)$  is sampled from a distribution of random vectors. Clearly,  $H_{SB}$  itself does not result in a preserved pointer basis or a preferred direction unless the distribution of  $\mathbf{b}$  is anisotropic. The effective Hamiltonian, on the other hand, can be engineered as

$$H_{SB,c} = h_z(\mathbf{b})\sigma_z + \epsilon[h_x(\mathbf{b})\sigma_x + h_y(\mathbf{b})\sigma_y], \quad (7)$$

where  $h_z(\mathbf{b})\sigma_z$  is the dominant term designed to preserve  $\{|0\rangle, |1\rangle\}$ . The small parameter  $\epsilon$  and the functional forms of  $h_x(\mathbf{b})$ ,  $h_y(\mathbf{b})$ , and  $h_z(\mathbf{b})$  will depend on the control sequence used for producing  $H_{SB,c}$ , as well as the details of the probability distribution. The calculation is straightforward for simple control sequences. In our notation,  $\omega_1 \equiv 2h_z(\mathbf{b})$  and  $|\langle 1|H_{\text{per}}|0\rangle|^2 \equiv h_x(\mathbf{b})^2 + h_y(\mathbf{b})^2$ . Our result for  $f_N$  translates into

$$f_N \approx 1 - \epsilon^2 \frac{[h_x(\mathbf{b})^2 + h_y(\mathbf{b})^2] \sin^2 [NT_c h_z(\mathbf{b})]}{4h_z(\mathbf{b})^2}, \quad (8)$$

as long as  $h_z(\mathbf{b}) \neq 0$ . Starting from  $f_0 = 1$ , the fidelity loss is thus at most  $\epsilon^2 h_z(\mathbf{b})^{-2} [h_x(\mathbf{b})^2 + h_y(\mathbf{b})^2]/4$ . Eq. (8) describes the fidelity dynamics for a single realization of the classical random field, whereas the actual open-system fidelity is the average of  $f_N$  over the distribution of  $\mathbf{b}$ . We shall use this approach in Sec. V A 1, to obtain approximate analytical results to be used in conjunction with our simulations of decoherence due to a quantum spin bath. Classical phase noise will also be relevant to the discussion of DD experiments on electron spins of P donors in Silicon in Sec. VII.

## B. Quantum Environment

In the quantum regime, Eqs. (2)-(3) describe a bipartite system, evolving under a Hamiltonian of the form

$$H_c = (H_{\text{dom}} + H_{B,c}) + \epsilon H_{\text{per}} \equiv H_D + \epsilon H_{\text{per}}. \quad (9)$$

While the dynamics generated by the unperturbed component  $H_D$  would affect a generic initial state preparation, it does *not* affect the fidelity of initial PSs. Consequently, in order to probe the fidelity dynamics of the

PSs only, the basic idea is to isolate the ‘‘PS-preserving dynamics’’ by effecting a transformation to a suitable interaction frame. As it turns out, this transformation will play a crucial role in our derivation, as it will provide the basis for applying von Neumann’s mean ergodic theorem (MET) [see Appendix A].

Let  $U_D \equiv \exp(-iT_c H_D)$  denote the propagator for the pure-bath and dominant interaction dynamics. The single-cycle propagator can then be factored as follows:

$$U_c \equiv \exp(-i\epsilon E)U_D, \quad (10)$$

$$\epsilon E = \epsilon T_c H_{\text{per}} + \sum_{m=1}^{\infty} \frac{b_m}{m!} [\epsilon T_c H_{\text{per}}, T_c H_D]_m + \epsilon^2 E^{[2+]},$$

where  $E^{[2+]}$  refers to corrections of second and higher order in  $T_c H_{\text{per}}$ ,  $b_m$  are the Bernoulli numbers, and  $[A, B]_m \equiv [\dots [A, B], \dots], B]$ , with  $B$  appearing  $m$  times [49]. Note that due to our assumption in Eq. (4),  $E$  is purely off-diagonal in the PS set, modulo the higher order  $E^{[2+]}$  terms. The propagator for  $N$  cycles thus reads

$$U_N = (U_c)^N = [\exp(-i\epsilon E)U_D]^N \equiv \tilde{U}_N (U_D)^N,$$

where the unitary operator  $\tilde{U}_N$  represents the propagator in the toggling frame generated by  $(U_D)^N$  and can be approximated by invoking a Magnus expansion [50]:

$$\tilde{U}_N \equiv \exp(-i\Omega_N), \quad \Omega_N = \epsilon \Omega_N^{[1]} + \epsilon^2 \Omega_N^{[2+]},$$

$$\Omega_N^{[1]} = \sum_{n=0}^{N-1} (U_D)^{-n} E (U_D)^n, \quad (11)$$

$$\|\Omega_N^{[2+]}\| = O(N^2 \|E\|^2) \approx O(T^2 \|H_{\text{per}}\|^2).$$

The time-discretization implied by the periodic evolution streamlines the application of von Neumann’s MET: the sum in Eq. (11) *projects  $E$  onto the commutant of  $U_D$*  and, as long as  $H_{\text{dom}}$  is non-degenerate, to that of  $H_{\text{dom}}$ . To implement this explicitly, let  $|j\rangle \otimes |b\rangle_j \equiv |j, b\rangle$  and  $\omega_{j,b}$  denote the eigenstates and eigenvalues of  $H_D$ , respectively, and let us expand  $E$  in the operator basis induced by  $|j, b\rangle$ , that is:

$$E = \sum_{j_1, b_1} \sum_{j_2, b_2} E_{j_1, b_1; j_2, b_2},$$

where  $E_{j_1, b_1; j_2, b_2} = \langle j_1, b_1 | E | j_2, b_2 \rangle | j_1, b_1 \rangle \langle j_2, b_2 |$ . Following Appendix A, we can partition  $\Omega_N^{[1]}$  in Eq. (11) into diagonal components in the  $|j, b\rangle$  basis, namely  $\Omega_N^{\parallel}$  (projected onto the commutant), and off-diagonal components in the  $|j, b\rangle$  basis, namely  $\Omega_N^{\perp}$  (projected outside the commutant). The diagonal components  $\Omega_N^{\parallel}$  vanish as a consequence of Eq. (4), since  $\Omega_N^{[1]}$  is related to  $H_{\text{per}}$  via commutators with  $H_{\text{dom}}$  which preserve the commutant structure [51]. The off-diagonal components  $\Omega_N^{\perp}$ , on the other hand, do affect the PS fidelities, but instead of growing linearly with  $N$  (or time  $T$ ), they are kept bounded by the MET. This is the fundamental feature of

PS preservation that guarantees a non-trivial long-time fidelity behavior. We can obtain an expression for the effective off-diagonal terms after averaging under the MET [Eq. (A1) in Appendix A]:

$$\Omega_N^\perp = \sum_{j_1 \neq j_2, b_1, b_2} \frac{1 - e^{i(N+1)T_c(\omega_{j_1, b_1} - \omega_{j_2, b_2})}}{1 - e^{iT_c(\omega_{j_1, b_1} - \omega_{j_2, b_2})}} E_{j_1, b_1; j_2, b_2},$$

where each term  $E_{j_1, b_1; j_2, b_2}$  is rescaled by a factor that is controlled by the inverse of the energy difference  $\omega_{j_1, b_1} - \omega_{j_2, b_2}$  and can be bounded independently of  $N$ . In summary, we can approximate the total propagator up to time  $T$  as:

$$U_N = \exp(-i\epsilon\Omega_N^\perp)(U_D)^N + O(\epsilon^2 T^2 \|H_{\text{per}}\|^2),$$

where

$$\|\Omega_N^\perp\| \leq \frac{\|E\|}{\sin(T_c \Delta/2)}, \quad \Delta \equiv \min_{j_1 \neq j_2} |\omega_{j_1, b_1} - \omega_{j_2, b_2}|.$$

Notice that transitions within the same  $|j\rangle$  sector do *not* appear at all, since  $E$  has no matrix elements within the same  $|j\rangle$  sector, ultimately due to Eq. (4).

We now proceed to obtain an approximate upper bound for fidelity loss of the designated PSs, along with conditions for its applicability. For simplicity, let us as before focus on an initial PS preparation in  $|0\rangle$ , that is:

$$\rho(0) = |0\rangle\langle 0| \otimes \rho_B(0), \quad (12)$$

where  $\rho_B(0)$  is an arbitrary state on  $B$ . The joint state after  $N$  cycles becomes

$$\rho(N) = \exp(-i\epsilon\Omega_N^\perp) \left[ |0\rangle\langle 0| \otimes \rho_B(N) \right] \exp(i\epsilon\Omega_N^\perp) + O(\epsilon^2 T^2 \|H_{\text{per}}\|^2),$$

where  $\rho_B(N) = U_D^N \rho_B(0) U_D^{-N}$ . To focus even more on the fidelity evolution of the initial state, we can further partition  $\Omega_N^\perp$  into parts that couple to  $|0\rangle$  and the rest:  $\Omega_N^\perp = \Omega_N^{(0)} + \Omega_N^{\text{rest}}$ . Up to corrections of  $O(\epsilon^2 \|\Omega_N^\perp\|^2)$ , we can then write

$$\rho(N) = \exp(-i\epsilon\Omega_N^{(0)}) \left[ |0\rangle\langle 0| \otimes \rho_B(N) \right] \exp[i\epsilon\Omega_N^{(0)}] + O(\epsilon^2 T^2 \|H_{\text{per}}\|^2) + O(\epsilon^2 T_c^2 \|H_{\text{per}}\|^2 / \sin^2(T_c \Delta/2)), \quad (13)$$

where we have bounded the corrections due to factoring  $\exp(-i\epsilon\Omega_N^\perp) \approx \exp(-i\epsilon\Omega_N^{(0)}) \exp(-i\epsilon\Omega_N^{\text{rest}})$  by  $O(\epsilon^2 \|\Omega_N^\perp\|^2)$  estimated by the final asymptotic term. Thus, the fidelity loss is governed by  $\epsilon\Omega_N^{(0)}$ . Let  $E_{|0\rangle} = \sum_{j \neq 0, b_1, b_2} (E_{0, b_1; j, b_2} + \text{h.c.})$ . Then we may bound

$$\|\Omega_N^{(0)}\| \leq \frac{\epsilon \|E_{|0\rangle}\|}{\sin(T_c \Delta_{|0\rangle}/2)}, \quad \Delta_{|0\rangle} = \min_{j \neq 0, b_1, b_2} |\omega_{j, b_2} - \omega_{0, b_1}|.$$

Physically, the ‘‘relevant gap’’  $\Delta_{|0\rangle}$  is the minimum energy difference between the  $|0\rangle$  sector and any other sector in

$H_D$ . In principle, the latter can be refined if detailed knowledge of the energy levels of  $H_{\text{dom}}$  and  $H_B$  is available. We also note that  $\|E_{|0\rangle}\| \leq \|E\| \approx T_c \|H_{\text{per}}\|$ .

Using the fidelity bounds in Ref. [52, 53] [see also Eq. (B1)], we can connect the operator norm of the effective Hamiltonian to fidelity loss. For small  $\epsilon$ , we have:

$$\begin{aligned} 1 - f_N &\leq \epsilon \|\Omega_N^{(0)}\| + O(\epsilon^2 T^2 \|H_{\text{per}}\|^2) + O(\epsilon^2 \|H_{\text{per}}\|^2 / \Delta^2) \\ &= \frac{\epsilon \|E_{|0\rangle}\|}{\sin(T_c \Delta_{|0\rangle}/2)} \\ &\quad + O(\epsilon^2 T^2 \|H_{\text{per}}\|^2) + O(\epsilon^2 \|H_{\text{per}}\|^2 / \Delta^2), \end{aligned} \quad (14)$$

which we can weaken and approximate to:

$$f_N \gtrsim 1 - \frac{\epsilon T_c \|H_{\text{per}}\|}{\sin(T_c \Delta_{|0\rangle}/2)}. \quad (15)$$

Notice that the fidelity bound in Eq. (14), is similar in structure to the semi-classical case bound from perturbation theory in Eq. (6), but is a weaker bound by a power of 2. While this is due to the coarse bounds for fidelity loss in terms of effective Hamiltonian from Ref. [53], we emphasize that these bounds have the advantage that they apply irrespective of the state of the environment. Also notice that the appearance of operator bounds guarantees a *polynomial dependence* on the number of subsystems  $n_B$  in the environment, as all system-environment operators can be written as sums of few-body interaction terms among the environment subsystems.

The bound on the fidelity loss in Eq. (14) is valid provided that two conditions are met: first,

$$\epsilon T \|H_{\text{per}}\| \ll 1, \quad (16)$$

which is a technical requirement for our approximations to be valid (in particular, for neglecting  $\Omega_N^{[2+]}$  with respect to  $\Omega_N^{[1]}$ ), and delineates the regime of applicability of MET in our analysis; and second,

$$\Delta \gg \epsilon \|H_{\text{per}}\|, \quad (17)$$

which is needed to ensure that no transition between the different pointer sectors occurs due to the perturbation. Both these requirements can be met by reducing  $\epsilon$ , the perturbation strength. Interestingly, we may interpret the gap condition in Eq. (17) as a simple *energetic protection* of coherence: PSs are protected indefinitely if the perturbation is too weak to cause a major transition among them. The role of a sufficiently gapped  $H_{\text{dom}}$  is precisely to ensure this energy barrier.

#### IV. CONSTRUCTIVE CONTROL PROTOCOLS

The results of the previous section provide a quantitative estimate on the *maximal* fidelity loss that PSs may incur, no matter how the latter happen to be produced. Ideally, the system starts with a nearly-perfect preparation (by means of a suitable quantum operation) in one

of the PSs, thus the fidelity  $f_0 = 1$ . As the control cycles are repeatedly applied, the fidelity will decay quickly for an initial transient [see Appendix B], but will eventually enter a “saturation” regime with a fidelity level lower-bounded by Eq. (15) once the number of applied cycles  $N$  is sufficiently large for the MET-averaging to kick in:

$$NT_c\Delta = T\Delta \gg 1.$$

This saturation regime will hold as long as the conditions in Eqs. (16)-(17) are satisfied. Within this picture, to engineer an arbitrary set of PSs, we need to:

- PS1: *Engineer the dominant cycle Hamiltonian*  $H_{\text{dom}}$  into the diagonal form of Eq. (3), so that the PS condition holds for the desired choice of  $\{|j\rangle\}_{j=0}^{p-1}$ , with  $1 \leq p \leq D_S - 1$ ;

- PS2: *Minimize the perturbation*  $H_{\text{per}}$ , by enforcing high modulation rates (that is, by reducing  $T_c$ ) and/or employing advanced control protocols similar to those in high-order DD [13, 15, 54] to get a higher fidelity bound [See Sec. V C]. Notice that this also implies that Eqs. (16) and (17) can be better satisfied and thus the desired PS set preserved to a *longer* guaranteed time.

In this Section, we describe how the tasks PS1 and PS2 can be achieved using unitary control pulses, for an arbitrary open-system setting in which  $H_{SB}$  and  $H_B$  are quantitatively unspecified (bounded) operators on  $\mathcal{H}_S \otimes \mathcal{H}_B$ . Although in principle continuous modulation schemes could be envisioned for this purpose, the pulsed control setting we focus on has the advantage to be mathematically straightforward while providing interesting connections to both DD theory and recent experiments. We begin by assuming that  $H_{SB}$  is *generic* – that is, it has *no* special symmetry hence no degeneracies – so that the engineered PSs and only those remain at high fidelity. We revisit this assumption in Sec. IV B.

### A. Generation of the Effective Hamiltonian

The control cycles in our construction are pulse sequences in which free evolution intervals of duration  $\tau_i$  are punctuated by application of *system* unitary operators  $P_i$ , so that  $T_c = \sum_{i=1}^n \tau_i$ . The operators  $P_i$  are assumed to be implemented as (nearly) instantaneous pulses by  $H_{\text{ctrl}}(t)$ . While in this section as well as in the examples of Sec. V we will also assume each pulse to be implemented perfectly, it turns out that such ideal-pulse assumptions are not essential as long as the unitary propagator does not change from cycle to cycle [See Sec. VI]. Similar to DD, the control pulses are so designed that  $P_i$  cancel each other:  $P_n \cdots P_1 = I_S$ . The overall unitary propagator for the cycle is an ordered product of pulse unitaries interlaced with evolution propagators  $\exp(-i\tau_j H_0)$  associated with the free intervals in which

$H_0 = H_{SB} + H_B$ . That is,

$$\begin{aligned} U_c(T_c) &= P_n \exp(-i\tau_n H_0) \cdots P_1 \exp(-i\tau_1 H_0) \quad (18) \\ &= Q_n^\dagger \exp(-i\tau_n H_0) Q_n \cdots Q_1^\dagger \exp(-i\tau_1 H_0) Q_1 \\ &= \exp(-i\tau_n Q_n^\dagger H_0 Q_n) \cdots \exp(-i\tau_1 Q_1^\dagger H_0 Q_1) \\ &\equiv \exp(-iT_c H_c), \end{aligned}$$

where  $Q_j = P_{j-1} \cdots P_1$  for  $n \geq j > 1$  and  $Q_1 = I_S$ . The effective cycle Hamiltonian  $H_c$  [Eq. (2)] can be approximated using a Magnus expansion:

$$T_c H_c = \sum_{j=1}^n \tau_j Q_j^\dagger H_0 Q_j + O(T_c^2 H_0^2). \quad (19)$$

In the special case of a uniform sequence, for which  $\tau_i \equiv \tau = T_c/n$ , we will simply denote the cycle in Eq. (18) by

$$f P_1 f P_2 \cdots f P_n,$$

where operations are now applied left-to-right and  $f$  stands for a free evolution interval.

The task PS1 then reduces to casting  $H_c$  in the form of Eqs. (2)–(3) for a designated PS set  $\{|j\rangle\}_{j=0}^{p-1}$ . Note that in *non-selective* (universal) DD schemes [9], a fixed choice of  $P_i$  (determined by the system dimensionality  $D_S$  and the symmetry of  $H_{SB}$ ) is used to cancel  $H_0$  (modulo pure-bath terms) up to various orders in  $\|T_c H_0\|$ . In this sense, PS1 is easier than DD, as it requires cancellation of far fewer terms in  $H_c$ . In fact, the minimum number of intervals in a cycle designed to completely cancel a generic  $H_{SB}$  is  $D_S^2$  [9, 55], while in contrast, as we shall prove below, the cycle for achieving PS1 for a complete pointer basis requires only  $D_S$  time slots. Achieving PS1 (and PS2) is, rather, close in spirit to *selective* DD, the price to be paid, however, being that the required control operations become necessarily *state-dependent*. A similar idea has been explored in Refs. [38, 54, 56], where “rotated” DD pulses are used to “lock” states in a particular one- or two- dimensional subspace of a two-qubit dissipative system. Note that selective (and encoded) DD for subspaces [57, 58] has also been specifically invoked for dynamical quantum error suppression, in alternative to non-unitary control strategies based on error-correcting codes [59]. A basic difference between the PS-engineering protocols that we will provide and the above-mentioned methods is the *dimension* of the preserved structures. Here, the preserved states correspond to *isolated points* (zero-dimensional manifolds) in the system Hilbert space, while by decoupling subspaces (or subsystems), the corresponding IPS corresponds to continuous manifolds of higher dimension.

As mentioned, the desired set of PSs may comprise any number  $p$  of orthonormal states. For clarity, we start with the task of engineering a single PS, follow with preserving a complete pointer basis, and finally provide a general recipe for engineering an incomplete pointer set that includes the former protocols as special cases.

### 1. Single Pointer State

Let  $|0\rangle$  be the solitary target PS ( $p = 1$ ). Define the unitary reflection operator

$$Q = 2|0\rangle\langle 0| - I_S. \quad (20)$$

Notice that despite the simple representation, implementing  $Q$  need not be simple, and we further comment on that in Appendix C. Consider a uniform pulse sequence consisting of two  $Q$  pulses separated by equal intervals of duration  $\tau = T_c/2$ . Using Eq. (19), one can verify that  $H_c$  for this sequence obeys the PS-condition in Eq. (3),

$$H_c = |0\rangle\langle 0| \otimes B_0 + H_{\text{per}} + I_S \otimes H_B,$$

where  $B_0$  is a bath operator and  $H_{\text{per}} = O(\tau\|H_0\|^2)$  [38, 54]. Since the latter can be made smaller by using shorter pulse intervals, the sequence will preserve  $|0\rangle$  with an arbitrarily high fidelity that can be maintained for a long time. Thus, PS1 and PS2 are both achieved by the control cycle  $fQfQ \equiv QQ$ .

If  $D_S = 2$ , the choice of  $|0\rangle$  determines a unique orthonormal state  $|1\rangle$  and Eq. (20) yields  $Q = |0\rangle\langle 0| - |1\rangle\langle 1| \equiv \sigma_z$ , resulting in a sequence that we shall simply denote  $ZZ$  henceforth. In a DD problem, this sequence is designed to suppress terms of the form  $\sigma_x \otimes B_X + \sigma_y \otimes B_Y$  in  $H_{SB}$ . In contrast, a universal DD sequence (such as  $XYXY$ ) is designed to cancel every possible term in  $H_{SB}$ , including  $\sigma_z \otimes B_Z$ . This generally results in an enhanced quantum memory where *all* states are preserved with a higher fidelity *initially*, but need not lead to a fidelity which is *maintained* for any particular state: even approximate eigenstates induced by  $XYXY$  are not apparent. Despite this distinction, in Sec. VA we will analyze the structure of  $H_{SB,c}$  for both sequences in detail, and show how the states  $|0\rangle$  and  $|1\rangle$  form a (accidental) pointer basis under the  $XYXY$  sequence as well.

### 2. Complete Pointer Basis

Let  $\{|j\rangle\}_{j=0}^{D_S-1}$  denote the set of  $p = D_S$  states we desire to preserve. Following [55], let us define the unitary operator  $\sigma_{D_S}$  as

$$\sigma_{D_S} = \sum_{j=0}^{D_S-1} \omega^{j+1} |j\rangle\langle j|, \quad \omega = e^{2\pi i/D_S}. \quad (21)$$

Direct calculation shows that for  $0 \leq i, j \leq D_S - 1$ ,

$$\sum_{k=0}^{D_S-1} (\sigma_{D_S})^{-k} (|i\rangle\langle j| \otimes B_{ij}) (\sigma_{D_S})^k = D_S \delta_{i,j} |i\rangle\langle i| \otimes B_{ii}.$$

Now consider a control cycle consisting of equal free intervals of length  $\tau = T_c/D_S$ , during which  $\sigma_{D_S}$  is applied  $D_S$  times, or  $f\sigma_{D_S} \cdots f\sigma_{D_S}$ . Thus,  $P_j = \sigma_{D_S}$  and

$Q_j = (\sigma_{D_S})^j$ . Using Eq. (19), the effective cycle propagator again takes the desired form of Eq. (3):

$$H_c = \sum_{j=0}^{D_S-1} |j\rangle\langle j| \otimes B_j + H_{\text{per}} + I_S \otimes H_B,$$

where, as before,  $\|H_{\text{per}}\| = O(\tau\|H_0\|^2)$ .

Note that the above sequence is by no means *uniquely* suited for the tasks PS1 and PS2. For example, sequences based on Hadamard arrays [60, 61] or products of  $\sigma_z$  Pauli matrices [62] can also be envisioned when the system is a collection of  $n_q$  qubits ( $D_S = 2^{n_q}$ ). Nonetheless, the sequence of  $\sigma_{D_S}$  operators described here is notable since it requires a *single pulse type*. As we shall see in Sec. VIB, this implies an extra degree of robustness against systematic control imperfections.

### 3. Incomplete Pointer Basis

Let  $\{|j\rangle\}_{j=0}^{p-1}$  denote the set of  $p < D_S - 1$  orthonormal states we wish to preserve (the case  $p = D_S - 1$  is equivalent to  $p = D_S$ , as already noted. The set  $\{|j\rangle\}_{j=0}^{p-1}$ , possibly along with other orthonormal states  $\{|j\rangle\}_{j=p}^{D_S-1}$ , forms an orthonormal pointer basis for  $\mathcal{H}_S$ . The construction described in the previous subsection can be readily modified to this scenario by introducing the following unitary pulse operator:

$$\sigma_{D_S}^p = \sum_{j=0}^{p-1} \omega^{j+1} |j\rangle\langle j| + \sum_{j=p}^{D_S-1} |j\rangle\langle j|, \quad \omega = e^{2\pi i/(p+1)}. \quad (22)$$

The 1st sum in Eq. (22) corresponds to a diagonal block of size  $p$  while the 2nd sum implies that  $\sigma_{D_S}^p$  acts as identity on  $\text{Span}\{|j\rangle\}_{j=p}^{D_S-1}$ . Consider a control cycle consisting of equal free intervals of length  $\tau = T_c/(p+1)$ , during which  $\sigma_{D_S}^p$  is applied  $p+1$  times, or  $f\sigma_{D_S}^p \cdots f\sigma_{D_S}^p$ . Using Eq. (19) with  $Q_j = (\sigma_{D_S}^p)^j$  for  $j = 1, \dots, p+1$ , we can verify that the effective cycle propagator for this sequence obeys the PS-condition in Eq. (3):

$$U_c = \exp[-iT_c(\sum_{j=0}^{p-1} |j\rangle\langle j| \otimes B_j + H' + H_{\text{per}} + I_S \otimes H_B)],$$

where, as required,  $H'$  annihilates  $\text{Span}\{|j\rangle\}_{j=0}^{p-1}$  and again  $\|H_{\text{per}}\| = O(\tau\|H_0\|^2)$ .

## B. Over-Symmetric Systems

In essence, PS engineering is about introducing and maintaining symmetries in the open-system Hamiltonian  $H_0$ , and indeed the protocols presented in Sec. IV A, in conjunction with the error bounds of Sec. III, succeed at achieving this goal if  $H_{SB}$  is generic, that is, not *over-symmetric*. The occurrence of *unwanted symmetries* can



cause two distinct problems. First and most importantly, they can result in energy degeneracies in  $H_{\text{dom}}$ . This will affect the perturbation theory requirements in our derivation of fidelity of PSs, since vanishing energy differences  $[\omega_j$  and  $\omega_{j,b}$  in Eqs. (6) and (15), respectively] will lead to a divergence in fidelity loss. In such cases, obviously applying the above control procedures may result in PSs that decay quickly. Second, another problem arises when a state *other* than the designated set  $\{|j\rangle\}_{j=0}^{p-1}$  happens to satisfy the PS condition in Eq. (3) due to additional symmetry. The intended PSs will then be preserved, but not exclusively so. In particular, decoherence-free subspaces or more general IPSs [63, 64] could exist/emerge in the presence of the control sequence that is used for engineering PSs.

Both the problematic scenarios of energy degeneracy and non-exclusivity of PSs can be remedied by modifying the control protocol so that  $H_0$  (and consequently  $H_c$ ) is suitably “de-symmetrized”. In practice, a situation of unconditional failure of the protocols described in Sec. IV A hints at hidden symmetries in the bare  $H_{SB}$  that persist in the effective cycle Hamiltonian  $H_{SB,c}$ , and need to be addressed by modifying the control protocol so that the transformation from  $H_0$  to  $H_c$  not only *introduces* the desired symmetry but also *removes* the undesired ones. A straightforward way in which such a desymmetrization can be obtained is to “turn on” an constant Hamiltonian on the system. For degenerate cases, an explicitly diagonal and non-degenerate control Hamiltonian can be applied, whereas for the undesired PSs an explicit coupling to yet another state (if available) will guarantee the desired desymmetrization. Another (pulsed) solution is to adjust the previous control protocols to remove the over-symmetry, as we describe next.

For simplicity, let us focus on a simple case where a single state  $|s\rangle$  is the source of the problem: it either shares energy eigenvalues with another fellow orthogonal PS, or it is an undesired PS. We will assume that another state  $|t\rangle$ , orthogonal to  $|s\rangle$  and the rest of the PSs, exists and that the following unitary (self-inverse) operator,

$$R = |s\rangle\langle t| + |t\rangle\langle s| + \sum_{i \neq s, i \neq t} |i\rangle\langle i|,$$

is available for control. Notice that  $R$  permutes the states  $|s\rangle$  and  $|t\rangle$ . Let the control cycle for generating the desired PSs [Sec. IV] be given by  $fP \cdots fP$ , where each pulse is originally applied  $n$  times. We will amend this sequence by concatenating [13] it with  $fRfR$ , that is,

$$[fRfR] P [fRfR] P \cdots [fRfR] P.$$

As a result, the number of pulses is now  $2n$  and they alternate between  $RP$  and  $R$ . Using Eq. (19), the cycle Hamiltonian becomes:

$$H_{SB,c} = \sum_{k=0}^{p-1} P^{-k} (RH_{SB}R + H_{SB}) P^k,$$

in which the inner expression  $(RH_{SB}R + H_{SB})$  effectively removes the degeneracy by “mixing” the states  $|s\rangle$  and  $|t\rangle$  as long as there is no further symmetry among them. Notice that, if the symmetry of  $H_{SB}$  is manifest, such as in a system exposed to collective noise, the operator  $R$  can be chosen from the outset to be a product of *unequal* unitary operations on each subsystem, which inevitably results in desymmetrization.

## V. ILLUSTRATIVE APPLICATIONS

### A. Single-Qubit Sequences

We begin by considering the task of engineering two arbitrary orthogonal states  $|0\rangle$  and  $|1\rangle$  as a pointer basis in a qubit. This basis defines the relevant Pauli operators, and the bare system-bath interaction  $H_{SB}$  can be correspondingly expanded as

$$H_{SB} = \sigma_x \otimes B_x + \sigma_y \otimes B_y + \sigma_z \otimes B_z,$$

for generic (traceless) operators  $\{B_\alpha\}$ . As before, let  $H_B$  be the bath internal Hamiltonian. Our goal is to thus preserve the eigenstates  $|0\rangle$  and  $|1\rangle$  of  $\sigma_z$  and, as mentioned, we shall both analyze the  $ZZ$  PS-protocol and the  $XYXY$  universal DD sequence. We can approximate the effective cycle Hamiltonian  $H_c$  using the Magnus expansion. For the  $ZZ$  sequence we have  $T_c = 2\tau$  and

$$H_{\text{dom}}^{[ZZ]} = \sigma_z \otimes B_z, \quad (23)$$

$$\begin{aligned} \epsilon H_{\text{per}}^{[ZZ]} &= \frac{\tau}{2} [\sigma_x \otimes B_x + \sigma_y \otimes B_y, \sigma_z \otimes B_z + H_B] \\ &+ O(\tau^2). \end{aligned} \quad (24)$$

The perturbative parameter in this setting is clearly proportional to  $\tau \|B_\alpha\|$ , where  $\alpha = x, y$ . For the  $XYXY$  sequence we have  $T_c = 4\tau$  and

$$\begin{aligned} H_{\text{dom}}^{[XYXY]} &= 4\tau \left( 2i\sigma_x \otimes [B_x, H_B] \right. \\ &\left. + \sigma_z \otimes (i[B_z, H_B] + \{B_y, B_x\}) \right), \end{aligned} \quad (25)$$

whilst  $\|H_{\text{per}}^{[XYXY]}\| = O(\tau^2)$ . For both sequences, higher-order corrections in  $\epsilon H_{\text{per}}$  will generically contain pure-bath terms, causing  $H_{B,c}$  to differ from the bare  $H_B$ .

Clearly,  $H_{\text{dom}}^{[ZZ]}$  has separable eigenstates of the form  $|i\rangle \otimes |b_i\rangle$  for  $i = 0, 1$ . For  $H_{\text{dom}}^{[XYXY]}$ , these eigenstates appear independently of  $B_x$  only if  $H_B = 0$ , that is, the bath is non-dynamical. Physically, the non-dynamical bath is a special but important case which provides, in particular, a prevalent approximation for decoherence of localized electronic spins in semi-conductors [28, 29]. Interestingly however, even for a generic *dynamical* bath,  $|0\rangle$  and  $|1\rangle$  are still preserved under the  $XYXY$  sequence. To see this we have to redefine  $H_{\text{dom}}$ . Recall that the fidelity preservation of PSs relies on the averaging caused by  $H_D$ , which since  $H_{\text{dom}}$  is made arbitrary small by

shrinking  $\tau$ , is dominated by  $H_B$ . Consider the bath-operators appearing in  $H_{\text{dom}}^{[XYXY]}$  in Eq. (25). The key observation is to realize that for any operator of the form  $[B_\alpha, H_B]$ , the component along the commutant of  $H_B$  vanishes (as long as  $B_\alpha$  is traceless), and hence these terms will act solely as perturbations according to Eq. (4). In contrast, the anti-commutator  $\{B_y, B_x\}$  will typically have a significant component along the commutant of  $H_B$ , and will break the symmetry in favor of the  $\sigma_z$  eigenstates. Thus, we may redefine the dominant Hamiltonian responsible for PSs as

$$H_{\text{dom}}^{[XYXY],\parallel} = 4\tau\sigma_z \otimes \{B_y, B_x\}, \quad (26)$$

which clearly still preserves  $|0\rangle$  and  $|1\rangle$ . A quantitative analysis of the resulting long-time fidelity follows.

### 1. Semi-Classical Environment: Analytical Results

The operators  $H_{\text{dom}}^{[XYXY]}$  and  $H_{\text{dom}}^{[ZZ]}$  can be calculated analytically within the semi-classical approximation of a static random-field environment described in Sec. III A. Phenomenologically, such a random magnetic field  $\mathbf{b} = (b_x, b_y, b_z)$  can approximate the effect of a nuclear spin environment interacting with a central spin qubit system under ensemble measurements [44]. In addition, as we shall describe in Sec. VI, systematic pulse imperfections can also formally mimic a classical always-on magnetic field. By invoking Eq. (8) with  $h_z(\mathbf{b}) = b_z$ , we obtain the ensemble-averaged fidelity loss:

$$\langle 1 - f_N \rangle_{\mathbf{b}} = \epsilon^2 \int \frac{[h_x(\mathbf{b})^2 + h_y(\mathbf{b})^2] \sin^2(NT_c b_z)}{4b_z^2} P(\mathbf{b}) d\mathbf{b}, \quad (27)$$

where  $P(\mathbf{b})d\mathbf{b}$  is the probability density associated with the distribution of  $\mathbf{b}$ . In the limit of  $N \rightarrow \infty$ , the rapidly oscillating term  $\sin^2(NT_c b_z)$  is smoothed out into a saturating (plateau) behavior. In contrast, for states other than the  $\sigma_z$ -eigenstates, the error grows to a *maximal* (unit) fidelity loss value.

It is illustrative to compute the average fidelity loss for the  $ZZ$  sequence with a specific distribution for  $\mathbf{b}$ . The calculation carries over to other sequences and can easily incorporate models of pulse imperfection reflected in different distributions for  $\mathbf{b}$  [see Sec. VI]. Let us assume, specifically, that the distribution is isotropic and the magnitude  $b$  is distributed according to a normal distribution  $P(b)$  with zero mean and standard deviation  $B$ . The expressions for  $h_x(\mathbf{b})$  and  $h_y(\mathbf{b})$  can be read off Eq. (24). The average fidelity loss can thus be calculated in a straightforward manner. For small  $N$ , we have:

$$\langle 1 - f_N \rangle_{\mathbf{b}} = \frac{2}{5} B^4 N^2 \tau^4 + O(N^3) \approx \frac{1}{10} B^4 T^2 \tau^2. \quad (28)$$

In this regime, the fidelity decays quadratically with both the elapsed time  $T$  and the control time scale  $\tau$ , also in line with general error bounds for cyclic DD [65]. In

contrast, for large  $N$ , the average fidelity loss saturates to a limiting (time-independent) value:

$$\langle 1 - f_\infty \rangle_{\mathbf{b}} = \frac{B^2 \tau^2}{12} + O(e^{-8B^2 N^2 \tau^2} N^{-2}) \approx \frac{B^2 \tau^2}{12}, \quad (29)$$

which is controlled by the product  $B\tau$ . The pattern of initial fidelity decay, followed by saturation, is the same pattern observed in exact numerical simulations of DD in quantum dots [28, 29]. In such a setting, the bath consists of a large number  $n_B$  of nuclear spins, each coupled to the central spin with a strength  $j_m$  and with

$$A \equiv \left( \sum_{m=1}^{n_B} \frac{j_m^2}{n_B} \right)^{1/2}$$

being a measure of the coupling strength [see also the upcoming Eq. (31)]. In the semi-classical limit, the environmental spins produce a classical Overhauser field. Using this analogy and the exact result for the asymptotic fidelity derived in Ref. [28, 29] for a maximally mixed bath initial state, that is,  $1 - f_\infty = \tau^2 A^2 n_B / 16$ , we can interpret the variance of the  $B$ -field as follows:

$$B^2 = \frac{3}{4} A^2 n_B. \quad (30)$$

Thus, we recover the polynomial dependence of the long-time fidelity of the engineered qubit PS's on  $n_B$ , as argued in Sec. III B on general grounds. This will be also verified in the upcoming numerical results [Figs. 3-4].

The initial decay of fidelity followed by a saturation (or freeze) regime is consistent with the more general semi-classical analysis carried out in [34–36]. The semi-classical approach also highlights an interesting connection to the Krylov-Bogoliubov method of averaging in classical dynamics [66], where an oscillatory motion is replaced by an average that yields approximate integrals of motion. In the quantum treatment, a similar behavior emerges from the theoretical model developed in Sec. III B, whereby the initial decay is followed by a bounded fidelity loss in the MET regime. Note that unlike the classical limit, after many oscillations (possibly when  $T$  no longer satisfies Eqs. (16) or (17)), fidelity may eventually drop, as the linear approximation implicit in the MET theorem (ignoring  $\Omega^{[2+]}$  terms) need no longer hold.

### 2. Quantum Environment: Exact Numerical Results

We illustrate our findings by means of exact numerical simulations where a spin qubit [ $\mathbf{S} = (S_x, S_y, S_z)$  spin operators] couples through Heisenberg interaction terms,

$$H_{SB} = \sum_{m=1}^{n_B} j_m \mathbf{S} \cdot \mathbf{I}^{(m)}, \quad (31)$$

to a quantum environment consisting of spin-1/2 particles [ $\mathbf{I}^{(m)}$  spin operators]. The (bare) internal Hamilto-

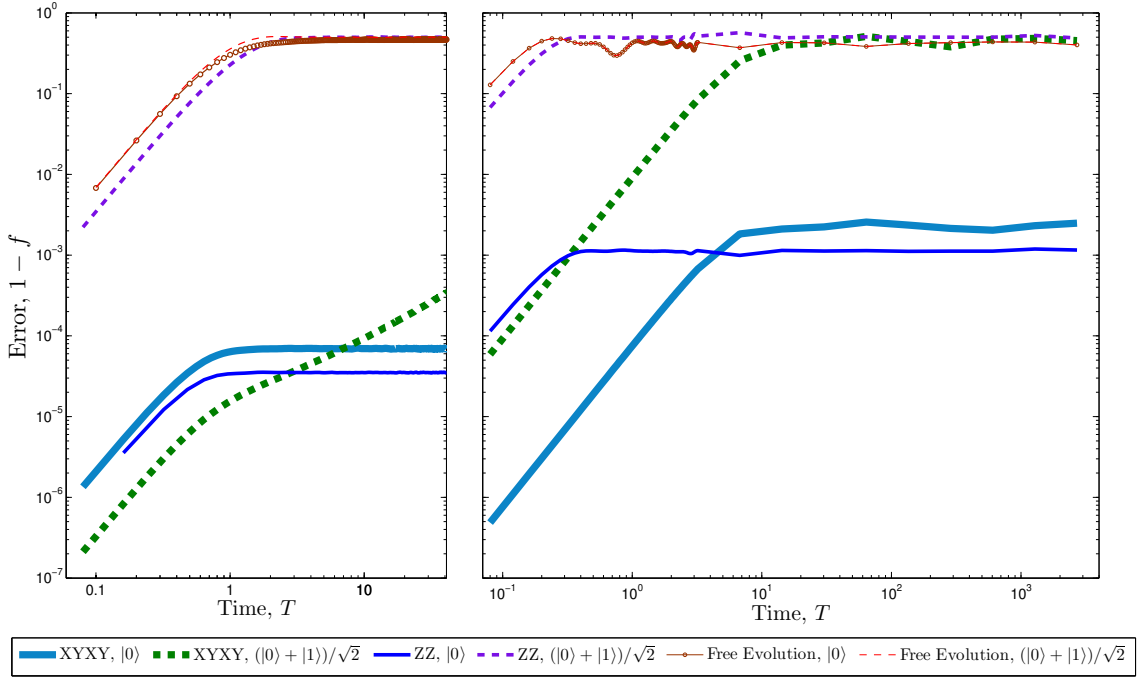


Figure 1: (Color online) Fidelity error ( $1 - f$ ) as a function of time for  $XYXY$  and  $ZZ$  sequences as well as the free evolution for  $|+X\rangle = (|0\rangle + |1\rangle)/\sqrt{2}$  and  $|+Z\rangle = |0\rangle$  initial states. Left:  $n_B = 15$  bath spins. Right:  $n_B = 8$  bath spins. In both cases the bath is non-dynamical ( $\beta = 0$ ), and the pulse interval is set at  $\tau = 0.01$  in arbitrary units. In order to allow for a comparable effective  $B$ -field [Eq. (30)] and error range, the maximum coupling  $|J_L| = 1$  ( $|J_R| = 4$ ) in the left (right) panel, respectively, with time kept in units of  $1/J_L$  in both cases. The difference in the time spans is due to practical limitations. Note that here and in the figures that will follow, the time axis is sampled non-uniformly to emphasize the interesting features of each time series without using too many data points. The sample points are connected by lines as a visual aid.

nian of the spin bath is taken to be of dipolar form:

$$H_B = \sum_{m=1}^{n_B} \sum_{k < m} \beta_{mk} (I_x^{(m)} I_x^{(k)} + I_y^{(m)} I_y^{(k)} - 2I_z^{(m)} I_z^{(k)}). \quad (32)$$

The coupling constants  $j_m$  between the system spin and each bath spin are arbitrarily generated by (uniformly) randomly sampling between  $-J$  and  $J$ . Similarly, the coupling constants  $\beta_{mk}$  between each two bath spins are randomly chosen between  $-\beta$  and  $\beta$ . We also assume that initially the bath is in a fully mixed state.

Fig. 1 compares the fidelity loss of different initial preparations under free evolution and under the  $ZZ$  and  $XYXY$  sequences designated to preserve  $|0\rangle \equiv |+Z\rangle$  and  $|1\rangle \equiv |-Z\rangle$ . Specifically, the system is prepared either as  $|+Z\rangle$  (intended as a PS) or  $|+X\rangle = (|0\rangle + |1\rangle)/\sqrt{2}$  (not intended as a PS). We observe that for the free evolution or for state  $|+X\rangle$ , the fidelity loss approaches a maximal value corresponding to a completely mixed state. Degradation is significantly faster for the free evolution and  $ZZ$  with  $|+X\rangle$  and considerably slower for the  $XYXY$  (with  $|+X\rangle$ ), as DD will nonetheless universally extend coherence times. In fact, the state  $|+X\rangle$  in the model with the larger environment (left panel) did not reach the maximal loss state within the simulation time under the  $XYXY$  sequence. On the other hand, with either

the  $ZZ$  or  $XYXY$  sequence, the desired PS  $|+Z\rangle$  is preserved with high fidelity after the initial transient is over. This initial decay is expected to occur before the MET regime kicks in and is approximately described by Eq. (28). Notice that the value of fidelity is non-trivially bounded after the initial decay, and furthermore it converges smoothly to a saturation value for all engineered PSs in Fig. 1. The saturation behavior is in agreement with the semi-classical result in Eq. (29). We also point out that the initial fidelity loss values depicted in Fig. 1 correspond to a the first period of control, at  $T = T_c$ , which is expected to scale with  $\|T_c H_{\text{per}}\|^2$ .

Fig. 2 depicts the change in fidelity of the preserved state  $|0\rangle$  by applying the sequences at different pulse intervals  $\tau$ . As expected, faster modulations (smaller  $\tau$ ) results in a smaller perturbation strength and thus higher fidelities. For both sequences, the ratio  $\|\epsilon H_{\text{per}}/H_{\text{dom}}\| = O(\tau)$  determines the long-time fidelity loss [Eq. (15)], but the difference in the structure of  $H_{\text{per}}$  vs.  $H_{\text{dom}}$  in the two cases [Eqs. (23)–(25)] is responsible for the noticeable difference between the final fidelity saturation value, the  $ZZ$  sequence outperforming the  $XYXY$  DD protocol.

In Fig. 3, we directly probe the dependence of the limiting fidelity ( $1 - f_\infty$ ) on the pulse interval  $\tau$  of the applied sequences, for various randomly generated coupling patterns  $\{j_m\}$  [Eq. (31)]. We can readily verify

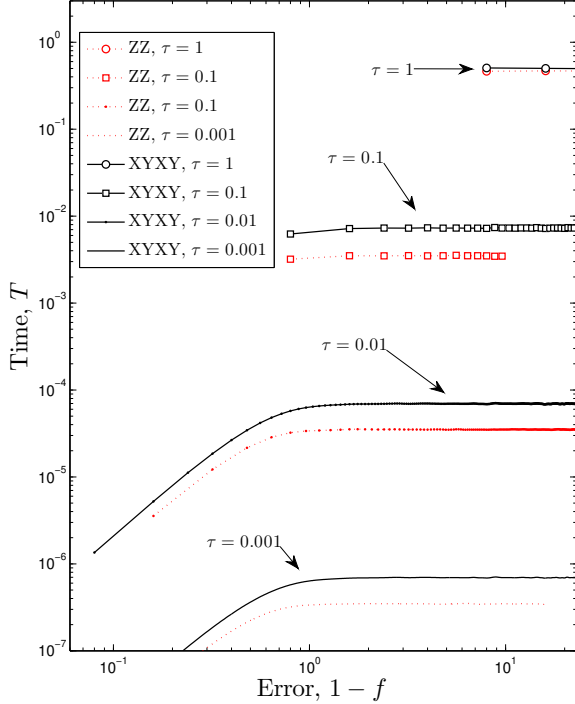


Figure 2: (Color online) Fidelity error ( $1 - f$ ) of  $|0\rangle$  as a function of time for  $XYXY$  and  $ZZ$  sequences with different pulse intervals  $\tau$ . The number of bath spins  $n_B = 15$  and the coupling is capped at  $|J| = 4$ .

that the observed fidelity loss scales with  $(A\tau)^2$ , as expected. In addition, Fig. 4 superposes the fidelity saturation values corresponding to environments of different size ( $n_B = 3, \dots, 8$ ), with the horizontal axis set to the bath-size-rescaled pulse interval  $A\tau n_B^{1/2}$  [28]. The fact that there is little variation in the curves confirms the validity of the semi-classical approximations leading to in Eqs. (29)-(30), and provides evidence that our simulation results may be reliably extrapolated to realistic environments with a far larger number of spins.

The numerical data presented thus far have addressed only “non-dynamical baths”, in which the internal coupling strength parameter  $\beta = 0$ . In the more general case where  $\beta \neq 0$ , the fidelity saturation value shows no significant dependence on  $\beta$  over the parameter range we explored. Results are summarized in Fig. 5. The independence of saturation fidelity from  $\beta$  is expected within the validity of the MET regime as well as in the semi-classical approximation. On the other hand, the value of fidelity loss *right after the initial cycle* does depend on  $\beta$ , and more strongly so for  $XYXY$  than  $ZZ$ .

Finally, note that for initial states other than  $|X+\rangle$  that are closer to  $|Z\pm\rangle$  PSs, the fidelity loss is smaller than the fidelity loss for  $|X+\rangle$ . In Fig. 6, we compare the relative survival of initial states in the  $xy$ -plane of

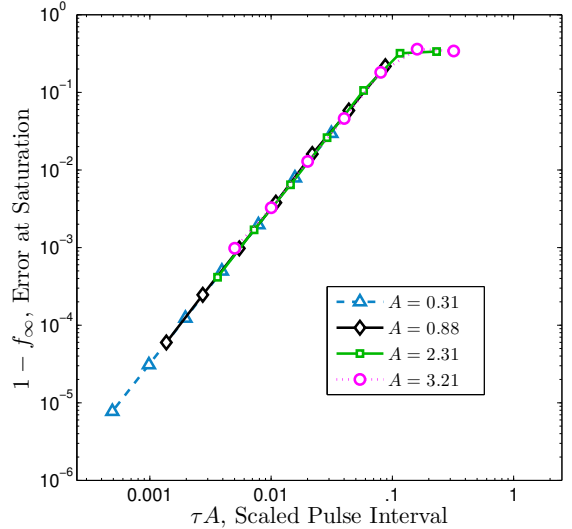


Figure 3: (Color online) Long time (saturated) fidelity error ( $1 - f_\infty$ ) as a function of rescaled interval  $\tau A$  for preserving  $|0\rangle$  with the  $ZZ$  sequence, and  $A = (\sum_{m=1}^{n_B} j_m^2/n_B)^{1/2}$ . The expression  $1 - f_\infty = 0.95(\tau A)^{1.99}$  [not shown in the figure] is a power-law fit to the series with the smallest  $A$ . The number of bath spins  $n_B = 8$  and  $H_B = 0$ . The overlapping curves correspond to randomly generated coupling patterns between the system qubit and the bath spins.

the Bloch sphere,  $|\psi\rangle = \cos(\theta/2)|0\rangle + \sin(\theta/2)|1\rangle$ , for various values of  $\theta$  for free evolution and the sequences  $XYXY$  and  $ZZ$ , respectively. We have defined the *relative survival* of a state as the inverse ratio of its long time fidelity loss and the maximal fidelity loss, that is,  $\xi(|\psi\rangle) \equiv (1 - f_{\min})/(1 - f_\infty(|\psi\rangle))$ , where  $f_{\min} = 1/2$  for a qubit (corresponding to the fully mixed state). Clearly, the engineered PSs ( $\theta = 0$ ) enjoy the highest survival ratios for sufficiently small  $\tau$ 's [Eq. (29)], as intended. Also notice that significant difference between the engineered PSs and the other states is virtually non-existent in the free evolution.

## B. Bell-State Pointer Engineering

We next consider a two-qubit spin system, coupled to a spin-1/2 environment similar to the one described in the single-qubit case. The spin operators for the two qubits are now denoted by  $S^{(1)}$  and  $S^{(2)}$ , respectively. Each qubit interacts individually with the bath spin particles via a Heisenberg Hamiltonian, thus

$$H_{SB} = \sum_{k=1}^2 \sum_{m=1}^{n_B} j_{m,k} \mathbf{S}^{(k)} \cdot \mathbf{I}^{(m)},$$

where as before we take the  $j_{m,k}$  coupling constants to be sampled from a random distribution with  $\max_{m,k} |j_{m,k}| \leq J$ , and no additional symmetry is present (in particular,  $j_{m,1} \neq j_{m,2}$  for at least one  $m$ ).

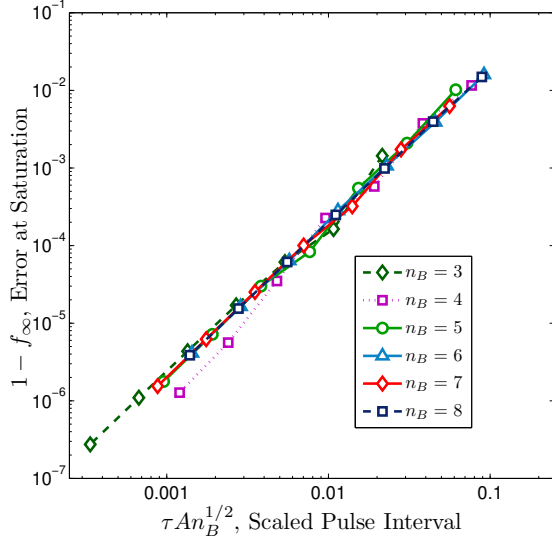


Figure 4: (Color online) Long time (saturated) fidelity error ( $1 - f_\infty$ ) as a function of bath-size-rescaled interval  $\tau A n_B^{1/2}$  for preserving  $|0\rangle$  with the ZZ sequence. The simulation used  $n_B = 3, \dots, 8$ , with randomly generated couplings. The remaining parameters are the same as in Fig. 3.

The bath internal dynamics is governed by the dipolar interaction described by Eq. (32), where we choose  $\beta = J$ . In addition, we also allow for an always-on Heisenberg interaction to be present among the qubits, that is,

$$H_S = K \mathbf{S}^{(1)} \cdot \mathbf{S}^{(2)}.$$

For concreteness, unless otherwise specified we shall match the intra-qubit interaction strength to that between the qubits and the environment spins,  $K = J$ . This corresponds to a coherent evolution between the qubits that is comparable to (and competing with) the interaction with the nuclear spin environment. We will use pulse sequences described in Sec. IV for preserving various sets of the Bell basis states:

$$\begin{cases} |\text{EPR}_0\rangle = (|01\rangle + |10\rangle)/\sqrt{2}, \\ |\text{EPR}_1\rangle = (|01\rangle - |10\rangle)/\sqrt{2}, \\ |\text{EPR}_2\rangle = (|00\rangle + |11\rangle)/\sqrt{2}, \\ |\text{EPR}_3\rangle = (|00\rangle - |11\rangle)/\sqrt{2}. \end{cases}$$

In particular, we engineer three sets of PSs with  $p = 1, 2, 4$  states chosen from the Bell basis. In what follows, all operators are given in the computational basis.

The sequence E1 is designed to preserve  $|\text{EPR}_1\rangle$  (singlet state) only. The cycle for E1 is based on the prescription given in Eq. (20), with  $|0\rangle$  being chosen as the EPR basis elements. With respect to the computational basis, the required control cycle consists then of two applications of the SWAP gate (see also [38]):

$$U_{\text{E1}} = \begin{pmatrix} 1 & 0 & 0 & 0 \\ 0 & 0 & 1 & 0 \\ 0 & 1 & 0 & 0 \\ 0 & 0 & 0 & 1 \end{pmatrix} = \exp[-i\pi \mathbf{S}^{(1)} \cdot \mathbf{S}^{(2)}] e^{i\pi/4},$$

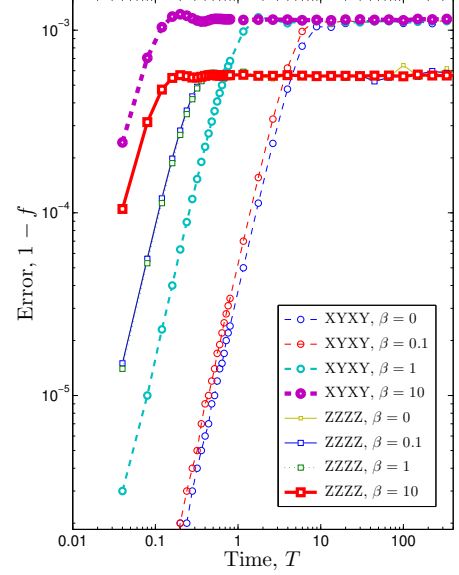


Figure 5: (Color online) Fidelity error ( $1 - f$ ) of  $|0\rangle$  as a function of time for XYXY and ZZ sequences with different scales of environmental couplings  $\beta$  in units of  $J$ . The interval is fixed at  $\tau = 0.01/J$ . Notice that for larger values of  $\beta$  the data series become almost indistinguishable. The number of spin baths  $n_B = 8$ .

Clearly, this operation can be implemented by the Heisenberg exchange interaction.

Similarly, the sequence E2 is designed for preserving  $\{|\text{EPR}_1\rangle, |\text{EPR}_2\rangle\}$  only, and is constructed using Eq. (22). The cycle for E2 consists of 3 applications of the unitary operation  $\sigma_{p=2, D_S=4}$  which, upon changing from the Bell to computational basis, takes the form

$$\begin{aligned} U_{\text{E2}} &= \begin{pmatrix} \frac{1+i\sqrt{3}}{4} & 0 & 0 & \frac{-3+i\sqrt{3}}{4} \\ 0 & \frac{1-i\sqrt{3}}{4} & \frac{3+i\sqrt{3}}{4} & 0 \\ 0 & \frac{3+i\sqrt{3}}{4} & \frac{1-i\sqrt{3}}{4} & 0 \\ \frac{-3+i\sqrt{3}}{4} & 0 & 0 & \frac{1+i\sqrt{3}}{4} \end{pmatrix} \\ &= \exp\left[\frac{i4\pi}{3}(S_x^{(1)}S_x^{(2)} + S_z^{(1)}S_z^{(2)})\right], \end{aligned}$$

that is, in terms of an isotropic XZ Hamiltonian.

Finally, the sequence E3 is designed to preserve all four EPR states  $\{|\text{EPR}_i\rangle\}_{i=0}^3$  (recall that it would be impossible to preserve exactly 3 orthogonal states in a 4-dimensional Hilbert space, as the remaining basis element would also be inevitably preserved) and is constructed using Eq. (21). Upon transforming, again, to the computational basis, the cycle for E3 consists of 4

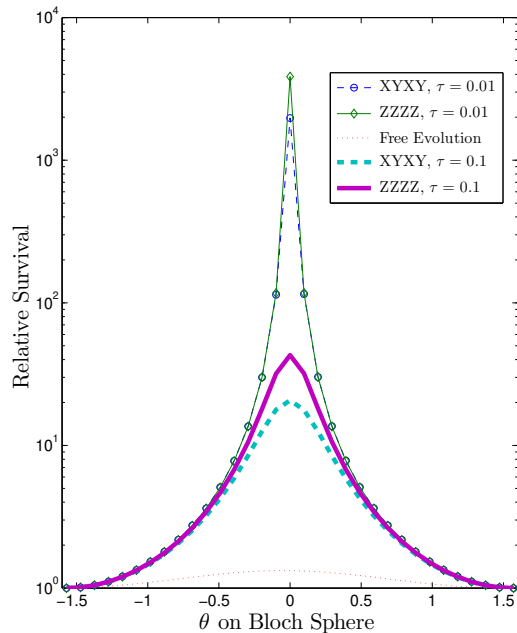


Figure 6: (Color online) Relative survival  $\xi(|\psi\rangle)$  (see text) as a function of time for various sequences across the Bloch sphere equator, with  $\theta = \pm\pi/2$  corresponding to  $|\pm X\rangle$ . Notice the high survival fidelity near the pointer basis element  $|0\rangle$  ( $\theta = 0$ ). The simulations used  $n_B = 8$  bath spins with  $H_B = 0$ .

applications of

$$\begin{aligned}
 U_{E3} &= \begin{pmatrix} \frac{i-1}{2} & 0 & 0 & \frac{i+1}{2} \\ 0 & \frac{1-i}{2} & \frac{i+1}{2} & 0 \\ 0 & \frac{i+1}{2} & \frac{1-i}{2} & 0 \\ \frac{-i-1}{2} & 0 & 0 & \frac{i-1}{2} \end{pmatrix} \\
 &= \exp[i\pi(S_x^{(1)}S_x^{(2)} + 2S_z^{(1)}S_z^{(2)})]e^{i\pi/4},
 \end{aligned}$$

Notice that all the sequences E1, E2, and E3 require two-body interactions. This is unsurprising since the Bell basis is entangled.

The sequences E1, E2, and E3 were numerically simulated for the two qubits coupled to a bath consisting of  $n_B = 15$  spins, and a set of 8 possible initializations (4 computational basis states and 4 Bell states) was evolved for each sequence. The simulation results for E1, E2, and E3 are summarized in Figs. 7, 8, and 9, respectively. Since in this case the contribution to  $H_{SB,c}$  due to the internal exchange Hamiltonian  $H_S$  need *not* be fully removed by the applied control, we have also plotted the purity loss  $(1 - \text{Tr}\rho_S^2)$  to factor out any remaining coherent evolution in the system and focus only on decoherence effects when needed. In all these figures, the eventual differentiation of the designated PSs from the others is clearly visible for each sequence.

Interestingly, as Fig. 9 reveals, the E3 sequence has a side-effect if  $K \neq 0$ . We note that the intra-qubit Heisenberg coupling  $H_S$  has the Bell states as its eigenstates. This implies that the E3 sequence effectively

leaves  $H_S$  invariant while it removes the terms in  $H_{SB}$  which would otherwise spoil the eigenstates. The net effect on the Bell states is as expected, they are preserved as PSs. However, the Heisenberg interaction implements a nontrivial swap-like evolution in the subspace spanned by  $\{|01\rangle, |10\rangle\}$ , while it acts as identity on the span of  $\{|00\rangle, |11\rangle\}$ . As a result, the E3 sequence enhances the internal system dynamics by removing the unwanted components of  $H_{SB}$ , and effectively resulting in a simple “logical gate” [17, 19]. This explains the oscillations in fidelity of  $\{|01\rangle, |10\rangle\}$  that are observed most prominently with the E3 sequence. These oscillations are absent when we focus on state purity (bottom panel in Fig. 9). Fig. 10 further highlights the difference in the evolution of fidelity and purity by explicitly contrasting the behavior of computational basis states in the case of interacting vs. non-interacting qubits, qualitatively confirming the above picture.

### C. Higher Order Sequences

The protocols introduced in Section IV and quantitatively illustrated in the above examples are all based on cancellation of the first order (time-linear) terms in the Magnus expansion for the effective cycle Hamiltonian  $H_c$ . Higher-order terms in Magnus expansion can also be removed. Cancellation of higher-order terms in the Magnus expansion is widely used in perturbative high-order DD procedures [13, 15, 16]. The timing and pulse type patterns used in such advanced DD schemes can be adapted to the task of PS-engineering if desired. While a detailed analysis is beyond our current scope, cancellation of higher-order Magnus corrections will result, for small enough control intervals, in further reducing  $H_{\text{per}}$  and thus the fidelity loss of the preserved PSs.

More concretely, consider a single qubit, where instead of using the ZZ sequences of Sec. V A, we apply the reflection  $Q$  ( $= \sigma_z$ ) follows the timing of Uhrig DD [15]. For higher-dimensional systems and for preserving a single PS, the protocol described in Sec. IV A 1 can likewise be modified to use a control cycle in which (as opposed to using two equal length pulse intervals) the pulse intervals are described by the Uhrig pattern [38]. For more than one PS, Uhrig DD is more difficult to adapt to PS-engineering. A possible construction may be devised in principle for  $D_S = 2^m$ -dimensional Hilbert spaces, by adapting the results in [67].

## VI. THE ROLE OF IMPERFECT CONTROL

Throughout the discussion so far, we have assumed control resources to be *perfect*, allowing for precise initialization of the system in (one of) the intended PS as well as exact implementation of all the required control operations. We now revisit these assumptions and analyze different ways in which limited control resources can

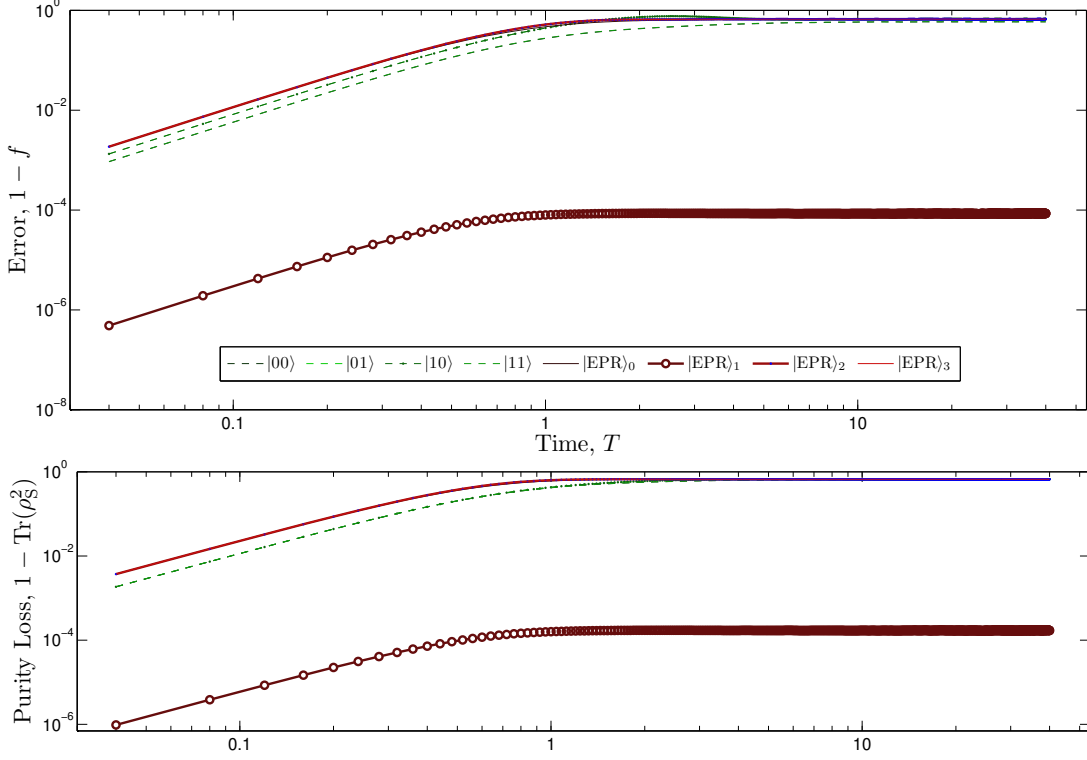


Figure 7: (Color online) Fidelity error ( $1 - f$ ) and purity loss ( $1 - \text{Tr}(\rho_S^2)$ ) for the  $E1$  sequence designated to preserve  $|\text{EPR}\rangle_1$  (see text). Different curves (some overlapping) correspond to initialization in the computational basis states and the Bell basis states, respectively. The number of bath spins  $n_B = 15$ , with  $\beta = J = K$ , and the pulse interval  $\tau = 0.01/J$ .

impact and/or modify the PS engineering problem.

### A. Preparation Errors

A deviation of the initial state from the intended pointer basis will propagate smoothly to the eventual fidelity of the system. Consider for concreteness a qubit, in which the  $\sigma_z$  eigenstates are the designated PSs, and let the initial preparation in the PS basis be described by

$$\rho_0 = \begin{pmatrix} 1 - \delta A & \delta(B + iC) \\ \delta(B - iC) & \delta A \end{pmatrix}, \quad (33)$$

where  $A$ ,  $B$ , and  $C$  are real numbers and the parameter  $\delta$  quantifies the error strength in the preparation of  $|0\rangle$ . For simplicity, let us further assume that  $|0\rangle, |1\rangle$  are preserved with the maximal fidelity 1, whereas eigenstates of  $\sigma_x$  and  $\sigma_y$  evolve to a maximally mixed state as  $T \rightarrow \infty$ . Using the linearity of quantum mechanics, we can show that at  $T \rightarrow \infty$ , the density matrix is given by

$$\rho_\infty = \begin{pmatrix} 1 - \delta A & 0 \\ 0 & \delta A \end{pmatrix}.$$

The fidelity loss in the evolution of  $\rho_0$  to  $\rho_\infty$  up to the leading order in  $\delta$  is given by:

$$1 - f_\infty = \frac{1}{2}\delta^2(B^2 + C^2) + O(\delta^3). \quad (34)$$

Eq. (34) implies that a state prepared in a sufficiently small neighborhood of a PS (in the convex set of possible states, including mixed ones) will evolve with a fidelity close to the maximal fidelity. In other words, starting with a slightly misprepared initial state and evolving under a PS-preserving protocol does result in lower fidelities but not a complete fidelity loss. In dynamical systems language, the PSs (and all the mixed states diagonal in the PS basis) are *Lyapunov stable* [32, 33]. The fact that the fidelities for states prepared near PSs remains lower than the PS-fidelities implies, however, that the dynamics is *not attractive*, consistent with the purely unitary nature of the applied control.

### B. Pulse Imperfections in Pointer-State Sequences

While a variety of imperfections can plague control Hamiltonians in real experiments, *systematic* pulse errors remain an important limiting factor for the achievable fidelities. As we now show, the latter can be incorporated in our theoretical framework as long as they result in a *constant* cycle propagator over the entire control duration. Let us reconsider a control cycle  $P_1, \dots, P_n$  designated for PS-engineering. Let  $U_{P_i}$  denote the propagator associated with the net evolution of the open system during (start to finish) the pulse  $P_i$ . The unitary operators

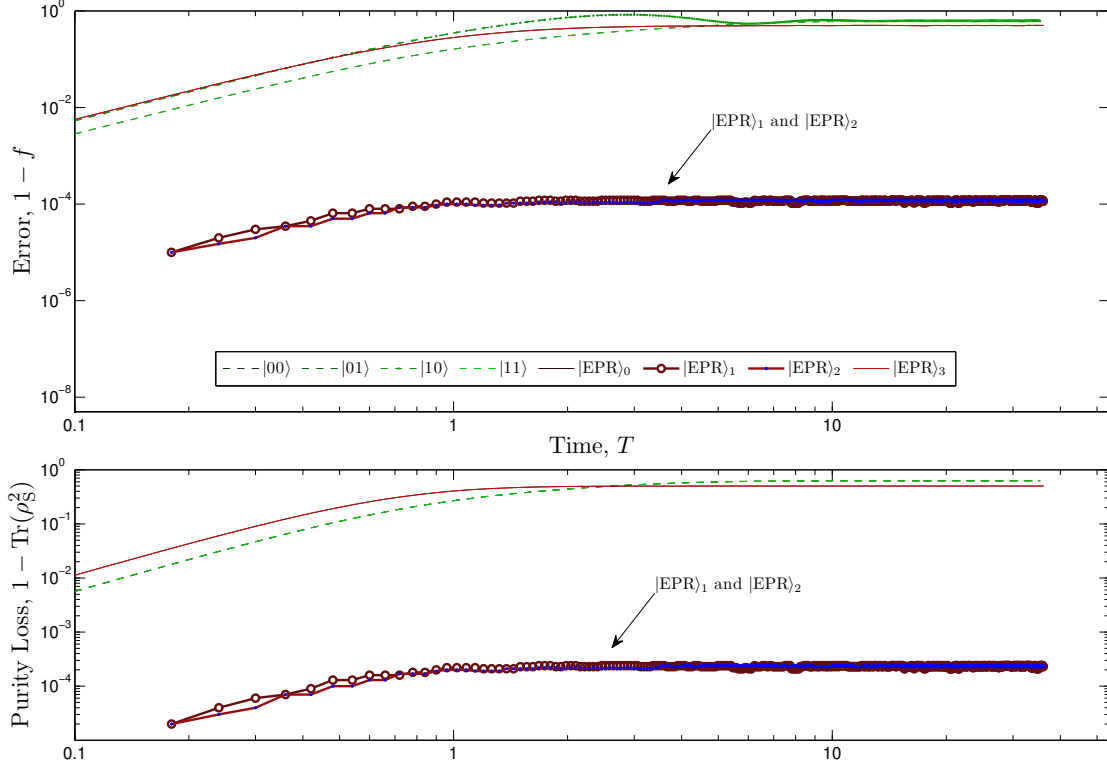


Figure 8: (Color online) Fidelity error ( $1 - f$ ) and purity loss ( $1 - \text{Tr}(\rho_S^2)$ ) for the  $E2$  sequence designated to preserve  $\{|\text{EPR}_1\rangle, |\text{EPR}_2\rangle\}$  (see text). Different curves (some overlapping) correspond to initialization in the computational basis states and the Bell basis states, respectively. The number of bath spins  $n_B = 15$ , with  $\beta = J = K$ , and the pulse interval  $\tau = 0.01/J$ . The apparently missing short-time fidelity/purity values for  $\{|\text{EPR}_1\rangle, |\text{EPR}_2\rangle\}$  are too close to 0.0 to be shown on the log scale.

$U_{P_i}$  are now approximations of the “ideal pulses”  $P_i$ :

$$U_{P_i} = P_i \exp(-iE_{P_i}), \quad (35)$$

where  $E_{P_i}$  is a Hermitian system-bath operator (the so-called “error action” [68]) that we refer to simply as pulse error. Following the notation of Sec. IV A, instead of Eq. (18) for ideal pulses, the cycle propagator thus reads

$$U_c = P_n \exp(-iE_{P_n}) \exp(-i\tau_n H) \\ \times \cdots P_1 \exp(-iE_{P_1}) \exp(-i\tau_1 H).$$

The error model described by Eq. (35) is general enough to encompass a large class of imperfections, such as finite-width-pulse errors (where  $E_{P_i}$  is a system-bath Hamiltonian depending on the pulse implementation) or, even in the narrow-pulse limit, rotation-angle and/or rotation-axis errors (with  $E_{P_i}$  acting on the system only). The pulse errors  $E_{P_i}$  are systematic in the sense that they only depend on the pulse  $P_i$ . This results in a fixed (constant) cycle propagator over the whole control duration, making it still meaningful to use an effective cycle Hamiltonian  $H_c$  up to the total time  $T$ . Letting  $\varepsilon \equiv \max_j \|E_{P_j}\|$  and

using the Magnus expansion, we may write [cf. Eq. (19)]:

$$T_c H_c = \sum_{j=1}^n \tau_j Q_j^\dagger H_0 Q_j + \sum_{j=1}^n Q_j^\dagger E_j Q_j \\ + O(T_c^2 H_0^2) + O(n T_c H_0 \varepsilon) + O(n^2 \varepsilon^2), \quad (36)$$

where we have used  $E_j$  for the error associated with the  $j$ -th pulse in the sequence, and we have explicitly shown the dominant linear terms while denoting the higher-order contributions by asymptotic expressions.

The protocols for engineering PSs discussed in Sec. IV are all based on bringing  $H_c$  to obey the PS-condition of Eq. (3), where  $\sum_j \tau_j Q_j^\dagger H_0 Q_j$  plays the role of  $H_{\text{dom}}$  and all the remaining terms are gathered into  $H_{\text{per}}$ . Clearly, the errors associated with pulse imperfections ( $E_{P_j}$ ) generally belong to  $H_{\text{per}}$ . Thus, while the task PS1 (ensuring PSs) can be achieved as before, the task PS2 (ensuring higher fidelity PSs) will depend on the quality of the pulses applied, as well as on access to shorter pulse intervals and/or more advanced control cycles. Recall, however, that in the protocols described in Sec. IV, a *single pulse type* ( $\sigma_{p,D_S}$ ) is used throughout the sequence, therefore only a single error per pulse appears in Eq. (36):  $E_{P_j} \equiv E_P$  for all  $j = 1, \dots, n$ . Remarkably, for such single-pulse-type protocols, the term



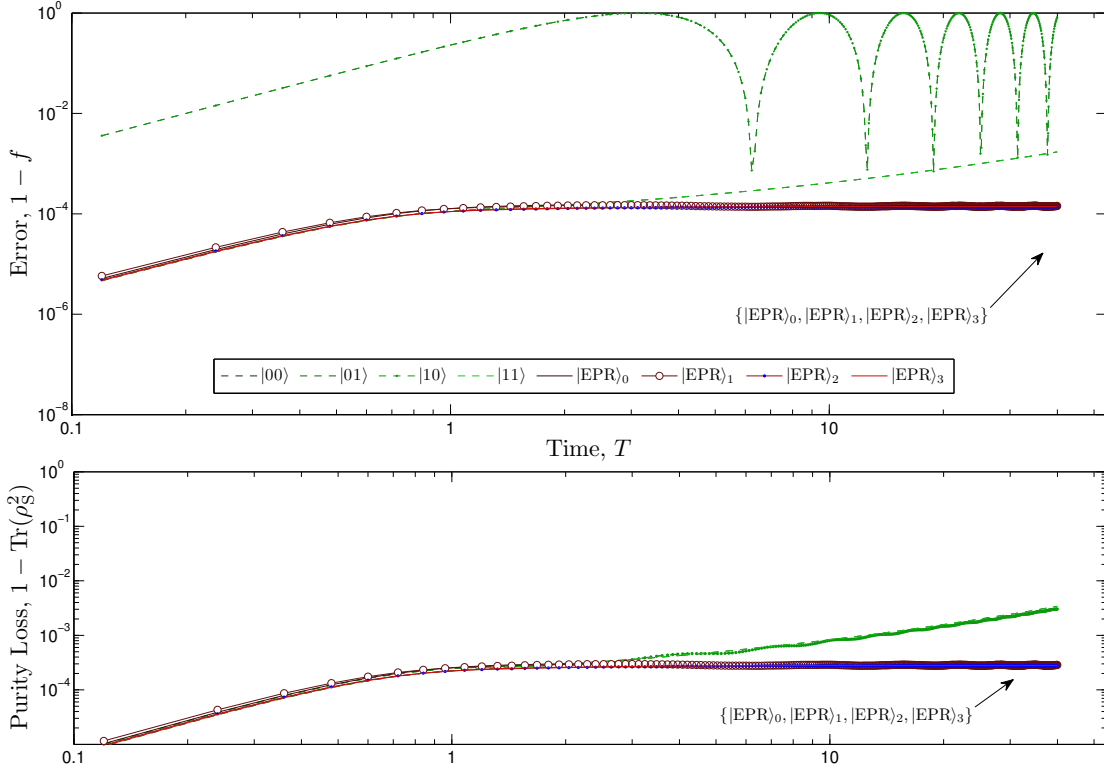


Figure 9: (Color online) Fidelity error ( $1 - f$ ) and purity loss ( $1 - \text{Tr}(\rho_S^2)$ ) for the  $E3$  sequence designated to preserve the complete Bell basis (see text). Different curves (some overlapping) correspond to initialization in the computational basis states and the Bell basis states, respectively. The number of bath spins  $n_B = 15$ , with  $\beta = J = K$ , and the pulse interval  $\tau = 0.01/J$ .

$\sum_j Q_j^\dagger E_j Q_j = \sum_j Q_j^\dagger E Q_j$  can actually be included in  $H_{\text{dom}}$ , and is *not* a perturbative correction. This leaves

$$T_c H_{\text{per}} = T_c H_{\text{per}}^{(0)} + O(n T_c H_0 \varepsilon) + O(n^2 \varepsilon^2), \quad (37)$$

where  $H_{\text{per}}^{(0)}$  refers to ideal pulses, and thus results in additional robustness compared to protocols that employ different pulse types.

The crucial implication of the redefinition of  $H_{\text{dom}}$  vs.  $H_{\text{per}}$  in Eqs. (36) and (37) is that although this will generally imply a worse fidelity lower-bound [cf. Eq. (15)] for a PS-protocol implemented with imperfect pulses, such imperfections will *not* result in a degradation of fidelity with time. This simple yet practically important point is quantitatively illustrated in Fig. 11 for a single qubit interacting with a spin bath as in Sec. V A. Specifically, we have analyzed the combined effect of rotation-angle and rotation-axis errors in preserving the state  $|0\rangle$  the  $ZZ$  protocol: the pulse error is characterized by letting  $E_P \equiv \eta(e_x \sigma_x + e_y \sigma_y + e_z \sigma_z)$ , where  $\eta \in [0, \pi]$  characterizes the over-rotation strength, and  $e_x, e_y, e_z$  are arbitrary (but fixed for all the data points) numbers randomly sampled from  $[-1, 1]$  which characterize the axis misalignment. The observed *robustness of the engineered PSs* with respect to systematic pulse errors is in sharp contrast to the behavior of DD protocols where repeating control cycles with faulty control tends to constantly degrade state fidelities for an arbitrarily chosen state [22].

## VII. POINTER STATES FROM IMPERFECT DECOUPLING SEQUENCES

In Sec. V A, we showed that the *imperfect cancellation* associated with single-qubit universal DD sequences results in the accidental generation of PSs. For instance, the  $XYXY$  sequence leads to a pointer basis in which the  $Z$  eigenstates are preserved and, as shown in the previous section, can survive without significant fidelity loss even in the presence of systematic control errors. Interestingly, however, even in situations where decoupling is theoretically exact, PSs can still emerge from *imperfect pulses*. This manifests in a strongly state-dependent degree of stability after many DD cycles, as recently demonstrated in the context of DD experiments using the electron spin resonance (ESR) of phosphorus donor spins in silicon, see in particular the data in Fig. 2 of [22] and Fig. 1 of [30]. In this Section, we show how the emergence of these stable states can be naturally re-interpreted and analyzed within our general framework, in terms of the emergence of a PS-supporting effective Hamiltonian.

The system under consideration is described in detail elsewhere [22, 30]. For a given spin  $S$ , in a frame that rotates with the electron's Larmor frequency, the bare Hamiltonian describing the interaction between each  $P$  electron spin and the nuclear spin bath can be approxi-

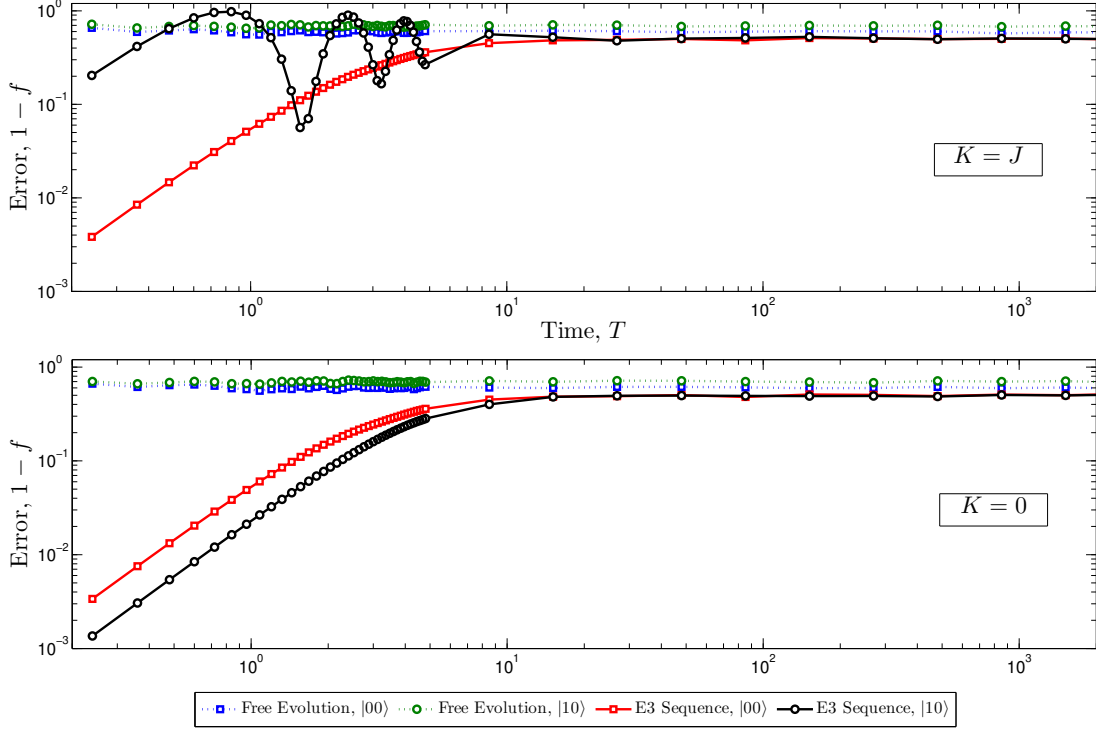


Figure 10: (Color online) Comparison between the evolution of  $|01\rangle$  and  $|00\rangle$  under free evolution and the  $E3$  sequence (see text) for  $K = J$  (exchange-coupled qubits,  $H_S \neq 0$ ) vs.  $K = 0$  (non-interacting qubits,  $H_S = 0$ ). The number of bath spins  $n_B = 8$ , with  $\beta = J$ , and the pulse interval  $\tau = 0.01/J$ . Notice the oscillations of  $|01\rangle$  when  $K \neq 0$ .

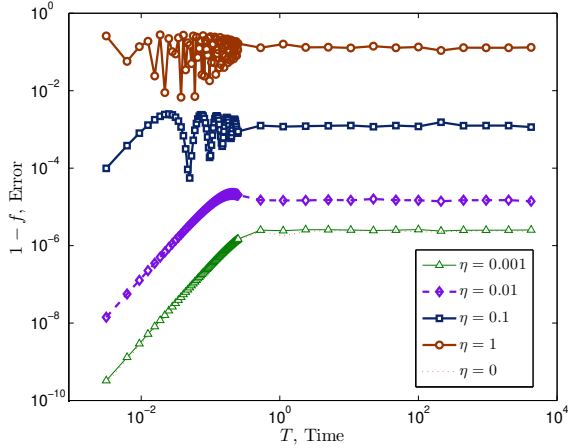


Figure 11: (Color online) Fidelity error ( $1 - f$ ) as a function of time for various over-rotation error strengths  $\eta$  for the  $ZZ$  sequence used for preserving  $|0\rangle$ . The error-free curve ( $\eta = 0$ ) is practically indistinguishable from the one at low error strength ( $\eta = 0.001$ ). The couplings  $\beta$  are in units of  $J$ , and  $\beta = J$ . The pulse interval is fixed at  $\tau = 0.01/J$  and the number of bath spins  $n_B = 7$ .

where  $\gamma_e$  and  $b_z$  are the electronic gyromagnetic ratio and the total effective magnetic field, respectively. The latter accounts for the effect of the nuclear spin environment and the off-resonance error resulting from spatial inhomogeneity across the sample, both of which can be treated as a random variable static in time to a good approximation. Clearly, the above interaction Hamiltonian implies a “natural” pointer basis along the  $Z$  axis in the absence of control: besides the eigenstates of  $\sigma_z$ , other states will not be preserved. In the presence of perfect (instantaneous) pulses, a universal DD cycle (such as  $XYXY$  or  $XZXXZ$ ) removes  $H_{SB}$  exactly. However, in the actual experiments, the DD pulses are not ideal, and their imperfections can rapidly accumulate over time, eventually nullifying the expected preserving action of DD on the spin’s quantum state. Despite their destructive role in DD, pulse imperfections can in fact select PSs, provided that they are constant over time, although inhomogeneous across the sample [69]. For ESR experiments, where the pulses are indeed close to ideal, we can approximate them as unitary rotations, with the rotation axes and angles slightly differing from their nominal values. In particular, for  $X$  and  $Y$  pulses, following the notation of Refs. [22, 30] the actual evolution operators

imated semiclassically approximated by [See Sec. V A 1]

$$H_{SB} = \gamma_e S_z b_z,$$

describing the imperfect rotations are

$$U_X = \exp[-i(\pi + \epsilon_x)\left(\frac{1}{2}\vec{\sigma} \cdot \vec{n}\right)],$$

$$U_Y = \exp[-i(\pi + \epsilon_y)\left(\frac{1}{2}\vec{\sigma} \cdot \vec{m}\right)],$$

where  $\epsilon_{x(y)}$ , with  $\epsilon_x \approx \epsilon_x \equiv \epsilon$ , are small errors in the rotation angles, and  $\vec{n}, \vec{m}$  are the actual rotation axes slightly differing from their nominal directions along  $x$  and  $y$ , respectively, that is, we may write  $\vec{n} \equiv (\sqrt{1 - \eta^2 n_y^2 - \eta^2 n_z^2}, \eta n_y, \eta n_z)$  and  $\vec{m} \equiv (\eta m_x, \sqrt{1 - \eta^2 m_x^2 - \eta^2 m_z^2}, m_z)$ , with  $\eta \ll 1$ . The parameters  $\epsilon$  and  $\eta$  thus play the role of the perturbative parameter  $\epsilon$  in the previous sections. The simplified but realistic one-dimensional model derived for ESR on a Si:P sample [22, 30] suggests that the probability distribution for the rotation angle error is peaked around a value  $\epsilon_0 \geq 0$  and is given by  $P(\epsilon) = (1/2\epsilon_0)[3(1 - \epsilon/\epsilon_0)]^{-1/2}$ , with  $-2\epsilon_0 \leq \epsilon \leq \epsilon_0$ . The axis offsets  $\eta n_{y(z)}$  and  $\eta m_{x(z)}$  each follow a similar distribution peaked around  $n_0 \geq 0$ .

Using Eq. (2), we can formally define the effective cycle Hamiltonian  $H_c$  associated with applying the  $XYXY$  sequence at the inter-pulse interval  $\tau$  (with  $T_c = 4\tau$ ). By direct calculation, taking into account terms up to the second order in pulse errors, we obtain:

$$T_c H_c = \sigma_z [-2\eta(m_x + n_y) + (\epsilon^2/2) \cos b_z \tau]$$

$$- 2\eta(m_x + n_y) \{[(\epsilon/2)(1 + \sin b_z \tau) - \eta n_z \cos b_z \tau] \sigma_x$$

$$+ [\eta m_z - (\epsilon/2) \cos b_z \tau - \eta n_z \sin b_z \tau] \sigma_y \}.$$

From the above expression, one can see how the separation of  $H_c$  into the dominant and the perturbative term happens. As long as off-axis errors are present ( $\eta \neq 0$ , independently of whether rotation errors are present also), the dominant term is simply the first contribution,  $T_c H_{\text{dom}} = -2\eta(m_x + n_y) \sigma_z$ , with all remaining terms belonging to the perturbative Hamiltonian  $H_{\text{per}}$ , which is  $O[\eta \max(\epsilon, \eta)]$  and is not in any particular direction. Using the results of Sec. III A, we expect the fidelity loss of PSs ( $Z$  eigenstates) to be proportional to the square of the ratio of the perturbative to dominant Hamiltonian, and hence controlled by  $O[\max(\epsilon, \eta)]$ . In the case where  $\eta = 0$ , to the leading order in the perturbative parameters we have instead  $T_c H_c = (\epsilon^2/2)(\cos b_z \tau) \sigma_z$ . Thus, while it is formally necessary to redefine  $H_{\text{dom}}$  so that it includes second-order contributions, the generated PSs will still be the  $Z$  eigenstates.

The  $XZXZ$  protocol is equivalent to the  $XYXY$  one in the absence of pulse errors but when pulse errors are taken into account, the resulting effective cycle Hamiltonian becomes qualitatively different:

$$T_c H_c = \sigma_y [(\epsilon/2)(1 - \sin b_z \tau) - \eta n_z(1 - \cos b_z \tau)]$$

$$- [(\epsilon/2)(1 - \sin b_z \tau) - \eta n_z(1 - \cos b_z \tau)]$$

$$\times \{-\eta m_x \sigma_x + [(\epsilon/2)(1 + \cos b_z \tau) - \eta m_z$$

$$+ \eta m_z \sin b_z \tau] \sigma_z \},$$

where we took into account that  $Z$  pulses in ESR experiments are implemented as  $Z = XY$ , by using two closely spaced  $X$  and  $Y$  pulses [22]. Clearly, the dominant term is the one in the first row of the above equation, which includes only terms of the first order in the pulse errors, and implies that the  $Y$  eigenstates now emerge as the pointer basis. The perturbative correction is  $O[\max(\epsilon, \eta)^2]$  and is not in any particular direction. Again, the fidelity loss is proportional to the ratio of the perturbative to dominant Hamiltonian, and controlled by  $O[\max(\eta, \delta)]$ .

This analysis parallels the consideration of Sec. V A. Thus, it is not surprising that the qualitative conclusions about the character of the generated PS are in perfect agreement with the experimental and theoretical results reported in [22, 30]. A quantitative analysis would need to take into account additional factors, most importantly the need to average the fidelity bound over the probability distributions of the offsets and over-rotation errors [similar to Eq. (8)]. While additional technical analysis of these specific experiments goes beyond our current scope, the above clearly demonstrates how our general framework can be modified to include the PS generated by DD pulse imperfections in context of direct experimental relevance.

## VIII. CONCLUSION

We have provided general open-loop unitary control protocols for engineering the interaction between a finite-dimensional system and its environment in the non-Markovian limit, in such a way that a desired set of pure states can be maintained as effective pointer states (PSs) of the dynamics. Our constructive results are supported by analytical upper bounds for the fidelity loss of the engineered PSs, which allow for systematic improvement by simply employing faster and/or more elaborated control schemes. While similar in flavor to dynamical decoupling protocols for protecting arbitrary quantum superpositions, the methods presented and analyzed in this paper aim to provide *selective energetic protection* for a designated set of pure states and their *convex* combinations only, effectively allowing for the on-demand generation of a *robust classical memory*. The fact that PSs are protected via relative energy gaps in the interaction with the environment is manifest in the nature of our performance bounds, which rely on von Neumann mean ergodic theorem and simple perturbation theory. Physically, the key requirement is to synthesize an effective Hamiltonian with a desired “dominant” symmetry structure, and to reduce the “perturbing interactions” that would otherwise destabilize the state and thus reduce the fidelity.

At the expenses of making the control design state-dependent, the PS-engineering protocols we have introduced have distinctive advantages over general-purpose dynamical decoupling schemes, which become most transparent in the task of engineering complex quantum states in multi-qubit systems as PSs. While the task

of Bell-state engineering we have analyzed in depth provides a paradigmatic example in this respect, the ability to engineer arbitrary PSs can potentially be useful as a resource in quantum information processing and/or quantum metrology tasks. It is also worth stressing that the methods we have presented are directly accessible via pulsed control, but can be modified in principle to allow continuous-time protocols that still effectively transform the interaction with the environment. Ultimately, stronger controls or faster pulse rates are the basic resources we leverage in achieving high-fidelity PSs within our Hamiltonian open quantum system setting.

A number of further questions may be worth addressing. For instance, it may be interesting to examine whether the present framework can be extended to encompass the more general symmetry conditions that allow for *time-dependent* PSs, as recently considered in [70]. From a control-standpoint, the latter problem might in turn relate to the possibility of robust time-dependent state-tracking, rather than long-time state-preservation as examined here. Interestingly, the distance of a density operator has recently been invoked to quantify “quantumness” in the context of coherent energy transfer in biological systems [71]. It is both natural and intriguing to ask whether a perturbative mechanism similar to the one involved in the generation of stable PSs examined here may be brought to bear on the problem of further understanding long-lived quantum coherences in complex systems. Lastly, the energetic protection against decoherence enjoyed by the PSs may be ultimately connected to quantum noiseless subsystem codes. Thus, a natural (although possibly highly non-trivial) direction for exploration is whether the idea of an engineered fidelity guarantee can be viable for a subsystem code that can preserve genuine quantum information, as opposed to only classical information as for a PS basis.

### Acknowledgments

L.V. gratefully acknowledges support from the NSF through award No. PHY-0903727. It is a pleasure to thank Francesco Ticozzi and Winton G. Brown for insightful discussions during the course of this work. Work at Ames Laboratory was supported by the Department of Energy — Basic Energy Sciences under Contract No. DE-AC02-07CH11358.

### Appendix A: Mean Ergodic Theorem

Let  $U$  and  $X$  denote, respectively, a unitary operator and arbitrary bounded operator acting on the same Hilbert space. The *von Neumann’s Mean Ergodic Theorem* (MET) implies that the limit

$$\lim_{N \rightarrow \infty} \frac{1}{N} \sum_{n=0}^{N-1} U^{-n} X U^n \equiv X^{\parallel}$$

exists and satisfies  $[X^{\parallel}, U] = 0$  [72]. Note that convergence is implied in any inner product distance between operators that is invariant under the adjoint action  $X \mapsto U^\dagger X U$ . In the above form, the MET has also been invoked to formally relate DD to the quantum Zeno effect [73].

To visualize the theorem for a finite-dimensional system, consider the complete basis of eigenstates  $\{|\phi_i\rangle\}$  of  $U$  with eigenvalues  $e^{i\phi_i}$ . The operator  $X$  can be written in the basis of the  $E_{ij} = |\phi_i\rangle\langle\phi_j|$  operators. The latter are transformed according to

$$U^{-n} E_{ij} U^n \mapsto e^{in(\phi_i - \phi_j)} E_{ij}.$$

Consequently, as long as there is no degeneracy ( $\phi_i \neq \phi_j$  unless  $i = j$ ), we have

$$\frac{1}{N} \sum_{n=0}^{N-1} U^{-n} E_{ij} U^n = \frac{1}{N} \frac{1 - e^{i(N+1)(\phi_i - \phi_j)}}{1 - e^{i(\phi_i - \phi_j)}} E_{ij}, \quad (\text{A1})$$

where in the limit of  $N \rightarrow \infty$ , the r.h.s. approaches zero when  $i \neq j$  and 1 otherwise. Thus, only diagonal basis elements are preserved under averaging and the remaining ones are annihilated. These diagonal basis elements span operators that commute with  $U$ . Notice that the left-over terms with  $i \neq j$  in the limit of a shrinking minimum gap,  $\Omega = \min_{i \neq j} |\phi_i - \phi_j|$ , scale with  $1/(N\Omega)$ .

### Appendix B: Initial Fidelity Decay

While the goal of our scheme is long-time manipulation of coherence using periodically repeated control cycles, we can nonetheless approximate the initial short time behavior of the system. In what follows we assume that

$$N\delta \equiv NT_c \epsilon \|H_{\text{per}}\| \ll 1,$$

where  $N$  is the number of control cycles that have been applied to the system up to time  $T = NT_c$ . This allows to use the linear (in  $\delta$ ) component of the interaction picture propagator  $\exp(-i\Omega_N^{[1]})$  as a substitute for the propagator when PS fidelity is concerned. We can estimate the norm of the effective Hamiltonian  $\Omega_N^{[1]}$  even before using Eq. (A1), directly from Eq. (11) in the main text:

$$\|\Omega_N^{[1]}\| \leq N\|E\| \approx N\|H_{\text{per}}\| = N\delta.$$

The fidelity loss of the system after  $N$  cycles can be bounded starting from the following bound for the Uhlmann fidelity  $f_N^U = f_N^{1/2}$  [52]:

$$1 - f_N^U \leq D \left[ |0\rangle\langle 0|, \exp(-i\Omega_N^{[1]}) |0\rangle\langle 0| \exp(+i\Omega_N^{[1]}) \right],$$

where  $D[\rho_1, \rho_2]$  is the trace distance:

$$D[\rho_1, \rho_2] \equiv \frac{1}{2} \|\rho_1 - \rho_2\|_1.$$

We can then use  $(1 - f_N) \leq 2(1 - f_N^U)$  [following from  $1 - x \leq 2(1 - x^{1/2})$  for  $0 < x < 1$ ] and the general bounds in Ref. [53], to show that

$$1 - f_N \leq \exp(\|\Omega_N^{[1]} + O(N^2\delta^2)\|) - 1 \leq (e - 1)\|\Omega_N^{[1]}\| \leq (e - 1)N\delta, \quad (\text{B1})$$

where in the last step we used  $e^x - 1 < (e - 1)x$ , for  $x \leq 1$ . We have thus bounded the short-time fidelity loss in terms of a linear function of the number of cycles  $N$  for small  $N$ . Note that for a single cycle, a tighter fidelity bound can be given, directly in terms of the (bath-averaged) variance of  $H_{\text{per}}$  in the initial PS [29], leading to  $1 - f(T_c) \lesssim (\epsilon\|H_{\text{per}}\|)^2 T_c^2$ . For large values of  $N$ , the results of Sec. III are applicable instead.

### Appendix C: Implementing Arbitrary Reflections

Implementing the PS-preserving pulses defined in Sec. IV is straightforward provided that tunable control Hamiltonians diagonal in the pointer basis are available, that is, Hamiltonians of the form

$$H_{\text{ctrl}}(t) = \sum_{i=0}^{D_S-1} h_i(t) |i\rangle\langle i|,$$

Note that in principle, even a constant in time Hamiltonian which is diagonal in the pointer basis and has non-commensurate eigenvalues would suffice for generating any unitary which is diagonal in the pointer basis [74]. If, however, no such control Hamiltonians are available, the problem of producing the required pulse operators can be difficult.

In particular, the pulse operators used in our protocols can be entangling if the system is multipartite. For example, this was explicitly the case in the PS-protocols employed for Bell-state engineering, Sec. VB. Furthermore, note that the operator  $Q$  used in Sec. IV A 1 to preserve a single PS corresponds to a multiple-controlled-phase quantum gate, thus, generally, entangling operations are required also to preserve a single product state (say, an element of the computational basis). Interestingly, however, preserving all computational basis elements in a multiple-qubit system requires no entanglement. For example, consider the control cycle resulting from concatenating (nesting) the  $ZZ$  cycles acting on every qubit [13, 67], resulting in preservation of the computational basis as an engineered pointer basis. These ideas suggest possible connections to the quantum search algorithm [75], in which the oracle performs the same (entangling) operation  $Q$  to select a particular element in the computational basis.

- 
- [1] W. H. Zurek, Phys. Rev. D **24**, 1516 (1981).
  - [2] W. H. Zurek, Rev. Mod. Phys. **75**, 715 (2003).
  - [3] W. H. Zurek, S. Habib, and J.-P. Paz, Phys. Rev. Lett. **70**, 1187 (1993).
  - [4] A. Isar, Fortschr. Phys. **47**, 855 (1999).
  - [5] J. Eisert, Phys. Rev. Lett. **92**, 210401 (2004).
  - [6] S. Boixo, G. Ortiz, and L. Viola, EPL **79**, 40003 (2007).
  - [7] R. Blume-Kohout, H. K. Ng, D. Poulin, and L. Viola, Phys. Rev. Lett. **100**, 030501 (2008); Phys. Rev. A **82**, 062306 (2010).
  - [8] L. Viola and S. Lloyd, Phys. Rev. A **58**, 2733 (1998).
  - [9] L. Viola, E. Knill, and S. Lloyd, Phys. Rev. Lett. **82**, 2417 (1999).
  - [10] P. Zanardi, Phys. Lett. A **258**, 77 (1999).
  - [11] P. Wocjan, M. Roetteler, D. Janzing, and T. Beth, Quantum Inf. Comput. **2**, 133 (2002).
  - [12] L. Viola, Phys. Rev. A **66**, 012307 (2002).
  - [13] K. Khodjasteh and D. A. Lidar, Phys. Rev. Lett. **95**, 180501 (2005).
  - [14] G. Gordon, G. Kurizki, A. G. Kofman, and S. Pellegrin, Quantum Inf. Comput. **5**, 285 (2005).
  - [15] G. S. Uhrig, Phys. Rev. Lett. **98**, 100504 (2007).
  - [16] J. R. West, B. H. Fong, and D. A. Lidar, Phys. Rev. Lett. **104**, 130501 (2010).
  - [17] L. Viola, S. Lloyd, and E. Knill, Phys. Rev. Lett. **83**, 4888 (1999).
  - [18] L. Viola and E. Knill, Phys. Rev. Lett. **90**, 037901 (2003).
  - [19] K. Khodjasteh and D. A. Lidar, Phys. Rev. A **78**, 012355 (2008).
  - [20] K. Khodjasteh, D. A. Lidar, and L. Viola, Phys. Rev. Lett. **104**, 090501 (2010).
  - [21] See for example recent experimental work by M. J. Biercuk *et al.*, Nature **458**, 996 (2009); Damodarakurup *et al.*, Phys. Rev. Lett. **103**, 040502 (2009); Y. Sagi, I. Almog, and N. Davidson, Phys. Rev. Lett. **105**, 053201 (2010); C. Barthel *et al.*, *ibid.* **105**, 266808 (2010); C. A. Ryan, J. S. Hodges, and D. G. Cory, *ibid.* **105**, 200402 (2010); G. de Lange *et al.*, Science **330**, 60 (2010); B. Naydenov *et al.*, Phys. Rev. B **83**, 081201(R) (2011); D. J. Szwer, S. C. Webster, A. M. Steane, and D. M. Lucas, J. Phys. B **44**, 025501 (2011); A. Ajoy, G. A. Alvarez, and D. Suter, Phys. Rev. A **83**, 032303; J. Bylander *et al.*, arXiv:1101.4707; H. Bluhm *et al.*, Nature Phys. **7**, 109 (2011).
  - [22] A. M. Tyryshkin, Z.-H. Wang, W. Zhang, E. E. Haller, J. W. Ager, V. V. Dobrovitski, and S. A. Lyon, arXiv:1011.1903.
  - [23] L. Viola, E. Knill, and S. Lloyd, Phys. Rev. Lett. **85**, 3520 (2000).
  - [24] L.-A. Wu and D. A. Lidar, Phys. Rev. Lett. **88**, 207902 (2002).
  - [25] M. J. Biercuk, H. Uys, A. P. VanDevender, N. Shiga, W. M. Itano, and J. J. Bollinger, Phys. Rev. A **79**, 062304 (2009).
  - [26] H. Uys, M. J. Biercuk, and J. J. Bollinger, Phys. Rev. Lett. **103**, 040501 (2009).
  - [27] K. Khodjasteh, T. Erdélyi, and L. Viola, Phys. Rev. A **83**, 020305 (2011).
  - [28] W. Zhang, V. V. Dobrovitski, L. F. Santos, L. Viola, and B. N. Harmon, Phys. Rev. B **75**, 201302(R) (2007).
  - [29] W. Zhang, N. P. Konstantinidis, V. V. Dobrovitski, B. N. Harmon, L. F. Santos, and L. Viola, Phys. Rev. B **77**,

- 125336 (2008).
- [30] Z.-H. Wang, W. Zhang, A. M. Tyryshkin, S. A. Lyon, J. W. Ager, E. E. Haller, and V. V. Dobrovitski, eprint arXiv:10116417.
- [31] J. Wang and H. Wiseman, Phys. Rev. A **64**, 063810 (2001).
- [32] F. Ticozzi and L. Viola, IEEE Trans. Autom. Control **53**, 2048 (2008).
- [33] F. Ticozzi and L. Viola, Automatica **45**, 2002 (2009).
- [34] T. Prosen and M. Žnidarič, New J. Phys. **5**, 109 (2003).
- [35] T. Prosen and M. Žnidarič, Phys. Rev. Lett. **94**, 044101 (2005).
- [36] Y. S. Weinstein, J. Emerson, S. Lloyd, , and D. G. Cory, Quantum Inf. Proc. **1**, 439 (2003).
- [37] T. Gorin, T. Prosen, T. H. Seligman, and M. Znidarič, Phys. Rep. **435**, 33 (2006).
- [38] M. Mukhtar, T. B. Saw, W. T. Soh, and J. Gong, Phys. Rev. A **81**, 012331 (2010).
- [39] Our results are immediately applicable to finite-dimensional systems and environments. However, protocols for engineering a *finite* set of PSs can be applied to infinite dimensional *systems* and our derivation can be extended to unbounded environments in which the infinite modes are restrained by the introduction of a physical energy cut-off.
- [40] This roughly corresponds to replacing operators on the bath with  $c$ -numbers that commute. While in a strict sense our derivation requires a time-independent bare Hamiltonian (thus a *static* random field in the classical limit), we expect our results to remain applicable for *slowly fluctuating* random fields, in analogy to DD methods, see *e.g.* [25, 76, 77].
- [41] For a closed system, Eq. (4) simply means that  $H_{\text{per}}$  must be purely off-diagonal (or *residual* in the quantum freeze terminology of [34, 35]).
- [42] R. Bhatia, *Matrix Analysis*, no. 169 in Graduate Texts in Mathematics (Springer-Verlag, New York, 1997).
- [43] Note that the input-output fidelity  $f_N$  differs in general from the fidelity overlap  $F_N$  considered in the context of Loschmidt echoes studies [34, 35, 37],
- $$F_N \equiv \text{Tr}[\rho_S^{\text{dom}}(N)\rho_S(N)],$$
- where  $\rho_S^{\text{dom}}(N)$  is obtained by evolving solely under the unperturbed (dominant) Hamiltonian. The two quantities coincide in the case of interest of an initial eigenstate of  $H_{\text{dom}}$ .
- [44] I. A. Merkulov, A. L. Efros, and M. Rosen, Phys. Rev. B **65**, 205309 (2002).
- [45] V. V. Dobrovitski, H. A. D. Raedt, M. I. Katsnelson, and B. N. Harmon, Phys. Rev. B **90**, 210401 (2003).
- [46] W. Coish and D. Loss, Phys. Rev. B **72**, 125337 (2005).
- [47] W. Yao, R.-B. Liu, and L. J. Sham, Phys. Rev. B **74**, 195301 (2009).
- [48] L. Cywinski, W. M. Witzel, and S. D. Sarma, Phys. Rev. B **79**, 245314 (2009).
- [49] S. Klarsfeld and J. A. Oteo, J. Phys. A **22**, 2687 (1989).
- [50] A. Iserles, Notes of the AMS **49**, 430 (2002).
- [51] The assumption in Eq. (4) appears to be used for simplifying the algebra but it hinges upon the knowledge of the dominant Hamiltonian and its PS set. This will be crucial to examine the unintended PSs emerging in DD protocols, see Sec. V A.
- [52] C. Fuchs and J. van de Graaf, IEEE Trans. Inf. Theory **45**, 1216 (1999).
- [53] D. A. Lidar, P. Zanardi, and K. Khodjasteh, Phys. Rev. A **78**, 012308 (2008).
- [54] D. Dhar, L. K. Grover, and S. M. Roy, Phys. Rev. Lett. **96**, 100405 (2006).
- [55] P. Wocjan, M. Rötteler, D. Janzing, and T. Beth, Phys. Rev. A **65**, 042309 (2002).
- [56] M. Mukhtar, W. T. Soh, T. B. Saw, and J. Gong, Phys. Rev. A **82**, 052338 (2010).
- [57] L. Viola, E. Knill, and S. Lloyd, Phys. Rev. Lett. **85**, 3520 (2000).
- [58] L.-A. Wu, M. S. Byrd, and D. A. Lidar, Phys. Rev. Lett. **89**, 127901 (2002).
- [59] E. Knill and R. Laflamme, Phys. Rev. A **55**, 900 (1997).
- [60] J. A. Jones and E. Knill, Journal of Magnetic Resonance **141**, 322 (1999).
- [61] D. Leung, J. Mod. Opt. **49**, 1199 (2002).
- [62] Z.-Y. Wang and R.-B. Liu (2010), arXiv:1006.1601v4.
- [63] D. A. Lidar, I. L. Chuang, and K. B. Whaley, Phys. Rev. Lett. **81**, 2594 (1998).
- [64] E. Knill, R. Laflamme, and L. Viola, Phys. Rev. Lett. **84**, 2525 (2000).
- [65] L. Viola and E. Knill, Phys. Rev. Lett. **94**, 060502 (2005).
- [66] N. M. Krylov and N. N. Bogoliubov, *Introduction to Non-linear Mechanics* (Princeton University Press, 1949).
- [67] Z. Wang and R. Liu (2010), arXiv:1006.1601.
- [68] K. Khodjasteh and L. Viola, Phys. Rev. Lett. **102**, 080501 (2009).
- [69] Note that each spin undergoes a slightly different evolution when subjected to an imperfect DD pulse. Strictly speaking, in such a situation, a PS should be understood slightly differently. It is no longer a pure state describing a single quantum spin, but rather the density matrix describing an ensemble of identical spins. The component of this density matrix which remains stable under the action of the pulses has a diagonal form in the basis of stable states. Therefore, a set of PS  $|j\rangle$  can still be formally associated with it, although these PS do not describe an actual quantum state of a single spin. Alternatively, one may consider a quantum state of an ensemble of independent spins, and define a set of product PSs  $|J\rangle = \otimes_{k=1}^n |j\rangle_k$ , where  $k = 1, \dots, n$  indexes the spins belonging to an ensemble. In this case, we are dealing with  $2^n$  PSs of the spin ensemble.
- [70] H. Daneshvar and G. W. F. Drake, arXiv:1104.4405.
- [71] P. Nalbach, D. Braun, and M. Thowart, arXiv:1104.2031.
- [72] M. Reed and B. Simon, *Modern Methods of Mathematical Physics. Vol. 1. Functional Analysis* (Academic Press, 1978).
- [73] P. Facchi, D. A. Lidar, and S. Pascazio, Phys. Rev. A **69**, 032314 (2004).
- [74] M. A. Nielsen and I. L. Chuang, *Quantum Computation and Quantum Information* (Cambridge University Press, Cambridge, UK, 2000).
- [75] L. K. Grover, in *Proceedings of the twenty-eighth annual ACM symposium on Theory of computing* (ACM, New York, NY, USA, 1996), p. 212.
- [76] L. Faoro and L. Viola, Phys. Rev. Lett. **92**, 117905 (2004).
- [77] L. Cywiński, R. M. Lutchyn, C. P. Nave, and S. Das Sarma, Phys. Rev. B **77**, 174509 (2008).